Eidgenössische Technische Hochschule Zürich
Swiss Federal Institute of Technology Zurich

University of Zurich[UZH]

Amygdala and hippocampus oscillations in human fear conditioning

by
Veronika Shamova
Master's Thesis

Institute of Neuroinformatics
University of Zürich and ETH Zürich
Zürich, Switzerland

August 2018

Supervisors:
Dr. Valerio Mante
Dr. Dominik R. Bach

Table of Contents

List of Tables

List of Figures

Abstract

Theta and gamma oscillations underlie various cognitive functions in humans, particularly learning and memory. One of their roles is supporting associative learning and synchronization between brain regions during fear conditioning. Animal studies have shown that conditioned stimuli, which predict the arrival of aversive stimuli, modulate theta and gamma oscillations, but their role in human fear conditioning is less certain. The goal of this study was to elucidate the role of theta and gamma oscillations during cued fear conditioning in the amygdala and hippocampus of humans using intracranial electroencephalography.

Compared to safety cues, presentation of cues associated with aversive stimuli elicited a decrease in theta oscillations in the hippocampus and increases in low gamma power in the hippocampus and amygdala over time. In addition, there was a difference in oscillatory behavior of the anterior and posterior hippocampus, with fear conditioning modulating primarily anterior hippocampal oscillations. Over trials, amygdalar-hippocampal phase synchronization in the theta range decreased for both conditions, while synchronization in the high gamma range was enhanced for the conditioned stimulus. A previously developed probabilistic model of fear learning was also applied to the data, and expectation of the aversive stimulus correlated with theta power and phase synchronization between the amygdala and the hippocampus.

These findings support a potential difference between the roles of theta oscillations in rodent and human fear processing, consistent with previous observations in memory formation studies, and further establish the role of gamma oscillations in emotional memory consolidation. Impaired acquisition

of safety signals may underlie anxiety disorders, and establishing the behavior of oscillations during fear acquisition has potential clinical applications.

Introduction

1.1 Fear conditioning

Fear conditioning is a behavioural paradigm which involves learning predictors of aversive events. It was first formalized by Ivan Pavlov in 1927 and has since been widely used and modified (Pavlov, 1927). In classical conditioning, two types of stimuli are used: conditioned stimulus, which signals the arrival of an aversive stimulus (CS) and unconditioned stimulus (US). The unconditioned stimulus elicits an innate response, such as aversion from pain. The conditioned stimulus is initially a neutral cue or context, such as a certain color or sound. During the training phase, the subject is exposed to the US paired with the CS, and learns to associate the CS with the arrival of US. Associative learning only occurs if two conditions are met — contingency, which is how predictive the conditioned stimulus is, and contiguity, which is how close in time the presentation of the two stimuli occurs. In the testing phase, only the conditioned stimulus is presented and the learned fear is measured by a variety of conditional responses. Conditioned responses in animals include freezing, enhancement of the startle reflex and cardiac responses such as changes in heart rate and blood pressure. Humans also exhibit heart rate changes, potentiation of the startle response and an increased skin conductance response (Maren, 2001).

Fear learning can be separated into acquisition and expression, and it can also be extinguished via extinction. Acquisition represents the initial learning stage, expression refers to the retrieval of the already established

fear memory, and extinction is the loss of the conditioned response to the cue.

Fear extinction involves the formation of a new memory rather than the modification of the original CS-US association. This is supported by the existence of well-documented phenomena such as return of fear, which is the spontaneous reappearance of a conditioned fear response after extinction (Rachman, 1989).

A variation of classical fear conditioning uses two conditioned stimuli: CS+ and CS-, where the former predicts the arrival of a US, while the latter does not; this paradigm is referred to as differential fear conditioning. This paradigm allows the possibility of differentiating between a heightened generalized response to sensory stimuli and an associative response to the CS+ (Collins, 2000), and it also helps examine the acquisition of a "safety" signal, as opposed to a "threat" signal.

Many different regions play a role in fear conditioning, including the amygdala, hippocampus, prefrontal cortex and others. These regions and their roles in fear conditioning and extinction are discussed below.

1.1.1 Neural substrates of fear conditioning

Amygdala

The amygdala is located in the temporal lobe of the brain and it is commonly associated with emotional processing. It consists of several subregions, namely the central nucleus (CEA) and the basolateral amygdala (BLA), further subdivided into the lateral (LA) and the basal (BA) amygdala. Lesions of the amygdala disrupted both innate and conditioned fear responses, but also responses to reward, demonstrating its widespread contributions to emotional processing (Davis, 1992).

Different nuclei of the amygdala have distinct roles in fear conditioning. The lateral amygdala receives projections from sensory areas such as the thalamus and auditory cortices, while the central amygdala projects to regions such as the brainstem, implicated in invoking fear responses, though recent

studies have also implicated the central nucleus in acquisition of fear (Pare, 2004).

During fear learning, activity-dependent plasticity occurs within the amygdala: long-term potentiation was shown to occur in LA after fear conditioning (Rogan et al., 1997). Long-term potentiation is a neuronal mechanism of strengthening of synaptic connections, which is thought to underlie memory formation. Sensory inputs about the CS and US converge on the same population of neurons in LA, supporting its role in integrating the two stimuli and establishing the CS-US association (Bocchio et al., 2017). The BLA also influences memory formation in the hippocampus via its influence on stress hormones such as adrenaline (McGaugh, 2004), which leads to better recall and a more stable memory trace for emotionally arousing experiences such as fear.

The central nucleus of the amygdala was initially thought to contribute only to the expression of fear responses due to its projections to areas involved in generating defensive responses (Fanselow, 1994), but recent work has demonstrated the necessity of LA projections to the CEA for fear acquisition (Tovote et al., 2015). Lesion studies have shown the role of CEA and its targets in expression of conditioned fear responses such as freezing and blood pressure changes, although some responses do not directly depend on CEA (Pape and Pare, 2010).

The amygdala also participates in fear extinction. Intercalated cells of the amygdala, which are located outside of the nuclei, are necessary for fear extinction (Likhtik et al., 2008). These cells have inhibitory projections to the CEA, and receive projections from the BLA, making them a good candidate for modulating extinction learning. However, extinction in the amygdala is also modulated by other brain regions such as the medial prefrontal cortex (mPFC) and the hippocampus.

Hippocampus

The hippocampus is located in the medial temporal lobe and is involved in memory encoding and spatial navigation. The hippocampus receives nu-

merous projections from sensory areas, and it has been proposed that a contextual representation is formed in the HPC during fear learning, which is then associated with the US (Sanders et al., 2003).

The rodent hippocampus is divided into the ventral (vHPC) and dorsal (dHPC) hippocampus, and the human analogues for these structures are the anterior and posterior hippocampus, respectively. Generally, vHPC is involved in encoding the emotional aspect of information (notably, anxiety-related behaviors) and dHPC encodes the spatial information (Fanselow and Dong, 2010; Orsini and Maren, 2012), though dHPC also participates in contextual fear conditioning (Pape and Pare, 2010). Lesions of vHPC have been shown to impair fear expression as well as fear extinction in both cued and contextual fear conditioning (Sierra-Mercado et al., 2011), thought to be due to vHPC-BLA projections which modulate fear expression. Additionally, activation of BLA inputs to the vHPC was enough to increase anxiety-related behaviors (Felix-Ortiz et al., 2013), supporting its role in expression of fear.

The hippocampus also plays a role in extinction, with lesion studies showing impaired memory of extinction and fear generalization. Extinction is thought to depend on context representation: Sevenster et al. (2018) have demonstrated that a switch in context leads to a renewal of extinguished fear. Context-dependent extinction is also mediated by the prefrontal cortex (Kalisch, 2006).

Prefrontal cortex

The medial prefrontal cortex (mPFC) is thought to be responsible for cognitive control, among other functions (Miller and Cohen, 2001). A recent model has suggested that mPFC plays a role in determining the outcome of actions and comparing the actual outcome with the expected one (Alexander and Brown, 2011), which is relevant for fear learning, since it involves expectation of the US based on the CS.

The mPFC participates widely in fear conditioning, mainly via the infralimbic and prelimbic cortices. The prelimbic cortex has been shown to participate in fear expression, while the infralimbic cortex is involved in fear

extinction (Sierra-Mercado et al., 2011), although recent studies indicate that the separation of function between these regions may not be as clear-cut: the prelimbic cortex also participates in formation and consolidation of the fear memory (Courtin, 2013), and the infralimbic cortex was shown to contribute only to short-term expression of extinction (Arruda-Carvalho and Clem, 2015). The complex contributions of the prefrontal cortex to fear conditioning may depend on the communication with its downstream targets such as the amygdala, vHPC and the thalamus, and the engagement of different neuronal populations in these targets, both by direct projections and oscillatory synchrony.

Other regions and connections in the fear circuit

Several other regions have been shown to participate in fear conditioning. For example, periaqueductal gray (PAG), located in the midbrain, receives inputs from sensory areas, mPFC and the amygdala, among others, and participates in pain modulation and defensive behaviors (Fanselow, 1994). Lesions in ventral PAG attenuate conditional freezing both in short-term and long-term fear conditioning retrieval (Kim et al., 1993). Insular cortex, located within the cerebral cortex, projects to the amygdala and relays sensory informaton. Consciously perceived CS+ trials led to increased activity in this region, suggesting its role in awareness of threat (Critchley et al., 2002). The dorsal region of the anterior cingulate cortex (ACC), a part of the frontal lobe, is activated by the CS and the activation was correlated with the skin conductance response, suggesting its role in fear expression (Milad et al., 2007).

Many neuronal mechanisms and circuits are active during the acquisition, retrieval and extinction of the fear memory (Figure 1.1). However, the amygdala and the hippocampus play crucial roles in this process. In particular, Desmedt et al. (2015) proposed that the interactions between these two regions directly contribute to formation of either adaptive or maladaptive fear memories, with maladaptive memories thought to play a role in anxiety disorders and other conditions.

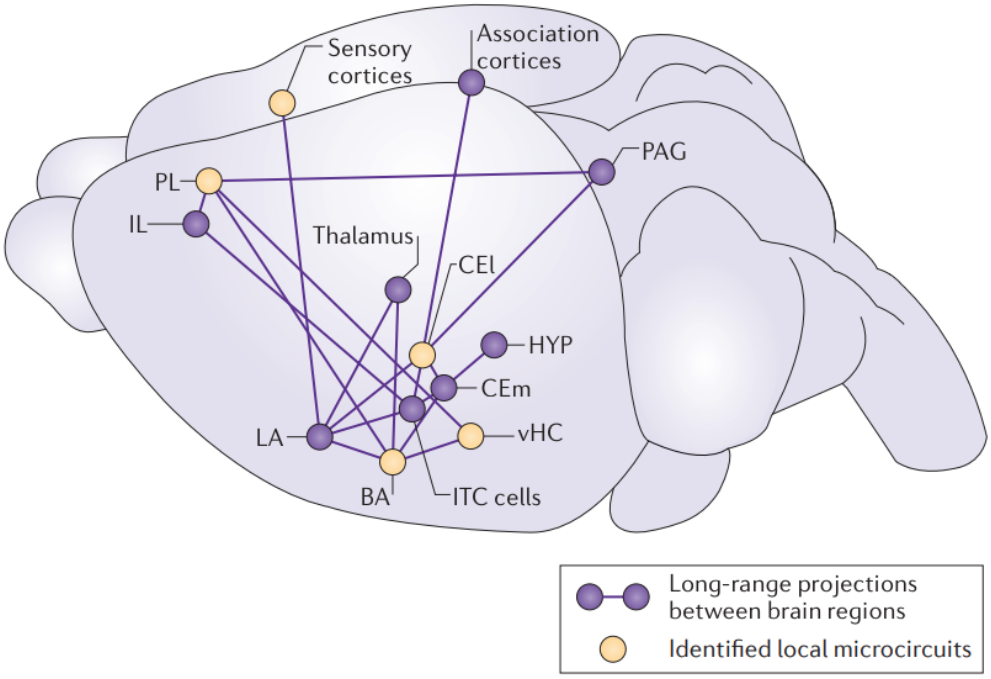

Figure 1.1: **Distributed brain regions involved in fear conditioning.** Various brain areas have been shown to participate in learning and expression of fear. In the amygdala, these regions are the lateral (LA), basal (BA) and central (CE) nuclei (with different contributions of the medial (CEm) and lateral (CEl) subregions), and intercalated cells (ITC). Other areas are the prelimbic (PL) and infralimbic (IL) cortices of the prefrontal cortex, ventral hippocampus (vHC), hypothalamus (HYP) and periaqueductal gray (PAG). Figure from Tovote et al. (2015).

1.1.2 Fear conditioning as a model of anxiety disorders

Fear conditioning has been utilized as a model of anxiety disorders. Anxiety disorders are characterized by the Diagnostic and Statistical Manual of Mental Disorders (DSM-5) as mental disorders that manifest in fear and anxiety that is excessive and out of proportion. These disorders include, but are not limited to, generalized anxiety disorder (GAD), characterized by excessive worry about various situations accompanied by physical symptoms; specific phobias, characterized by fear and avoidance of a specific object or situation; and social anxiety, characterized by fear and avoidance of social situations (American Psychiatric Association, 2013). The latest edition of the DSM includes post-traumatic stress disorder (PTSD) in a separate chap-

ter on trauma-related disorders, though it is also commonly referred to as an anxiety disorder.

Several aspects of fear conditioning have been found to be impaired in anxiety disorders, including impaired fear extinction (Milad et al., 2008; Sehlmeyer et al., 2011) and insufficient discrimination between the cue that predicts the aversive stimulus (CS+) and the safety cue (CS-), also referred to as fear generalization. In fear generalization, conditioned stimuli that never predicted the aversive cue also elicit a conditioned response. In part, generalization of fear is an adaptive tactic, ensuring that the organism can extrapolate threat predictions to cues that are not identical to the learned predictor. However, excessive fear generalization is a hallmark feature of anxiety disorders and presents a problem in everyday life (Dunsmoor and Paz, 2015).

Differential conditioning provides a way to study fear generalization, as it includes an conditioned stimulus that is never paired with an aversive cue (CS-). A meta-analysis by Duits et al. (2015) involved 44 studies on fear conditioning in anxiety disorders and found overall significant differences between fear responses to CS- in patients and healthy controls during acquisition, as well as a stronger fear response to CS+ in patients during extinction. Gazendam et al. (2013) have also found that individuals with high trait anxiety have impaired safety learning and show more pronounced fear responses to the safety cue CS- in comparison to healthy controls, further supporting the role of impaired fear acquisition and fear generalization in anxiety.

Generalization of the conditioned response is generally attributed to many areas, including the sensory cortices, the vmPFC, the amygdala and the hippocampus (Dunsmoor and Paz, 2015). In the hippocampus, fear generalization is thought to be related to impaired pattern separation; in the amygdala, generalization was shown to be related to distinct neuronal populations; and in the prefrontal cortex, synchronization between mPFC and BLA was related to the ability to discriminate between the safety and the threat cues (Kheirbek et al., 2012; Likhtik et al., 2014; Ghosh and Chattarji, 2015). The communication between areas involved in fear conditioning

is frequently modulated by oscillations, which have also been implicated in anxiety (Oathes et al., 2008; Miskovic et al., 2010; Adhikari et al., 2010).

1.2 Local field potentials and brain oscillations

Local field potentials (LFPs) represent the electric activity in extracellular space in the brain as recorded within the brain tissue with methods such as intracranial electroencephalography (iEEG). The current view of their origin holds that LFPs are comprised of various sources, including synaptic currents, Ca^{2+} spikes, intrinsic currents and resonances as well as high frequency action potential bursts. The shape of the neuron also influences its contribution to the LFP, with pyramidal neurons contributing the most due to the shape of their apical dendrites and to their spatial arrangement (Buzsáki et al., 2012). Local field potentials also reflect synchronized activity in the form of neural oscillations.

Oscillations are ubiquitous in nature, and they also arise in the human central nervous system. They were first described in the brain by Hans Berger, who observed the alpha wave (8-12 Hz) during normal waking activity (Berger, 1929). Other knowns rhythms include the beta (12.5 – 30 Hz), theta (4-8 Hz), gamma (30-80 Hz), and delta (0.5-4 Hz) waves. These rhythms are an evolutionarily conserved feature, evidenced by conservation of frequency bands and behavioural correlates across multiple species (Buzsáki et al., 2013); however, inter-species variations still exist, as discussed in Section 1.2.1.

Brain oscillations are implicated in numerous functions such as attention and memory (Jensen and Colgin, 2007), sensorimotor integration (Caplan et al., 2003) and navigation (Kahana et al., 1999), among others. Oscillations have also been reported to be the timing system of the brain, controlling the temporal coding – in particular, individual neurons have been found to phase-lock to theta and gamma oscillations, as well as delta oscillations in some regions (Jacobs et al., 2007). Theta and gamma oscillations in particular

have been implicated in emotional processing and fear conditioning, and their function and regions of origin are discussed in detail below.

1.2.1 Theta oscillations

Theta waves are low frequency oscillations in the brain. In rodents, they are defined in the range of 4 to 12 Hz, and further separated into two subtypes: type 1 (also known as atropine-resistant theta), which has a frequency around 8 Hz and above, and type 2 (atropine-sensitive) theta, which has a frequency between 4 and 8 Hz. Type 1 theta oscillations are associated with voluntary movement, while type 2 theta waves are seen with anxious apprehension and freezing (Kramis et al., 1975). In humans, 4-8 Hz oscillations are relatively transient, and some evidence exists that points to the fact that theta oscillations are slower in humans than in rodents: functionally similar oscillations occur at 4-8 Hz in rodents and at 1-4 Hz in humans (Jacobs, 2013), and slow theta oscillations centered at around 3 Hz in humans were found to be related to episodic memory formation (Lega et al., 2012).

There are several intrinsic sources of theta waves in the brain — initially, it was thought that the main contributors are medial septal inhibitory interneurons (Hangya et al., 2009), but there is also evidence for hippocampal theta oscillators that are independent of the medial septal nucleus (Goutagny et al., 2009). In the amygdala, cells of the basolateral complex of the amygdala have been shown to generate theta-range oscillations (Pape et al., 1998). Therefore, despite the existence of many oscillators in the brain, both the amygdala and the hippocampus generate intrinsic theta oscillations.

Theta oscillations have diverse functions in the brain. They have been implicated in memory: in mice, theta oscillations have been linked to long-term memory retrieval (Narayanan et al., 2007); in cats, theta rhythms (4.5 to 10 Hz) synchronize medial PFC activity during trace conditioning (Paz et al., 2008); in humans, enhanced 3 Hz theta oscillations in the hippocampus have been linked to successful memory encoding (Lega et al., 2012), and theta waves exhibit phase-phase coupling with gamma waves in the hippocampus during working memory tasks (Chaieb et al., 2015). Theta rhythms in the

hippocampus were also enhanced during a working memory task (4-8 Hz) (Axmacher et al., 2010). However, there is also evidence that successful episodic memory formation corresponds to a decrease in hippocampal theta oscillations (3-8 Hz) (Long et al., 2014). In addition, Greenberg et al. (2015) found that decreases in low theta activity in the temporal lobes and frontal cortex underlie associative memory encoding.

Another function of theta waves is temporal coding: in rats, theta cycles coordinate local circuit computations in the entorhinal-hippocampal system (Mizuseki et al., 2009) and synchronize mPFC-CA1 interactions during a spatial memory task (Jones and Wilson, 2005). Theta-gamma cross-frequency coupling has also been shown to participate in timing of neuronal events and form a memory code (Lisman and Jensen, 2013), further discussed in Subsection 1.2.3.

Fear conditioning (CS+ presentation in particular) has been found to induce theta responses in the lateral amygdala in rodents (Seidenbecher et al., 2003). It is hypothesized that the amygdala and the medial prefrontal cortex communicate via theta waves in order to evaluate potentially threatening stimuli (Likhtik and Paz, 2015). Theta frequency activity was also correlated between the mPFC and ventral hippocampus in anxiogenic environments such as an open field test, which is representative of innate anxiety in mice (Adhikari et al., 2010; Likhtik et al., 2014). Additionally, Lesting et al. (2011) have found increased theta-range cross-correlation between area CA1 of the hippocampus, LA and mPFC, but this coupling decreased over repeated retrieval sessions. Therefore, theta range synchronization might play a role in inter-regional communication during fear conditioning.

Theta rhythm plays a vital role in coordination and synchronized activity during fear conditioning. Nevertheless, no consensus exists on its precise mechanisms and frequencies across species. More evidence in humans is required to establish whether rodent fear conditioning findings could be directly extrapolated to humans.

Table 1.1 shows a comparison of various findings regarding theta oscillations during fear conditioning.

Study	Method	Species	Stage of learning	Findings
Paré and Collins (2000)	LFP	Cats	Retrieval	Increased firing of LA neurons, synchronization in the theta range during fear
Seidenbecher et al. (2003)	LFP	Mice	Retrieval	Increased synchronization in the theta range between CA1 and LA during CS+ presentation at 24 hours after conditioning
Pape et al. (2005)	LFP	Rats	Retrieval	Amygdala and hippocampus synchronize in the theta range (4-8 Hz) during retrieval of long-term fear memory
Adhikari et al. (2010)	LFP	Mice	Retrieval	vHPC theta increases in the open field (corresponding to innate anxiety)
Lesting et al. (2011)	LFP	Mice	Retrieval and extinction	Retrieval: theta activity in LA, mPFC and CA1, decreased theta synchronization between all areas over repeated retrieval. Extinction: increase in theta range cross-correlation between CA1 and mPFC, low cross-correlation between LA and CA1
Likhtik et al. (2014)	LFP	Mice	Retrieval	BLA and mPFC theta synchronization during CS- only in animals that discriminate between CS+ and CS-
Stujenske et al. (2014)	LFP	Mice	Retrieval	BLA gamma oscillations synchronize with mPFC theta during safety and with BLA theta during fear

McHugh et al. (2014)	LFP	Mice	Retrieval	CS+ increased theta oscillations (5-10 Hz), theta oscillations also increased over time between training days
Karalis et al. (2016)	LFP	Mice	Retrieval	Increased 4 Hz oscillations in the BLA during freezing associated with CS+ presentation
Taub et al. (2018)	LFP	Primates	Retrieval	Increased theta oscillations (4-8 Hz) after CS presentation and before US presentation
Sperl et al. (2018)	EEG-fMRI	Humans	Retrieval and extinction	Increased frontomedial activity in the theta range (4-8 Hz) at retrieval that correlated with amygdala activation, reduced theta power at extinction
Tzovara et al. (2018b)	MEG	Humans	Retrieval	Suppression of theta power (1-8 Hz) during CS+ presentation, increased hippocampus and amygdala interaction in the theta band in CS+ trials

Table 1.1: **Summary of electrophysiological studies of theta oscillations in fear conditioning.** A comparative table of studies of theta oscillations in the amygdala and the hippocampus during fear conditioning across animal species, electrophysiological methods and phases of fear conditioning

1.2.2 Gamma oscillations

Gamma waves are defined to be above 30 Hz in frequency and are observed in a number of brain regions, particularly in their engaged state. Similar to theta oscillators, gamma oscillators are typically inhibitory interneurons, with models involving cellular networks of various types of cells that give rise to gamma rhythms (Buzsáki and Wang, 2012).

Gamma activity has been associated with working memory load (Howard et al., 2003; van Vugt et al., 2010), perception and object representation (Tallon-Baudry

and Bertrand, 1999), and attention (Fries et al., 2001; Engel et al., 2001). It should be noted that aforementioned sources refer to oscillations ranging from 30 to 90 Hz. In addition to those oscillations, another gamma band has been defined, usually from 90 to 150 Hz, with some using a mid-frequency band between 50 and 90 Hz (Belluscio et al., 2012). Evidence exists for distinctive roles of slow and fast gamma, with slow waves participating in information retrieval, while fast waves are involved in information encoding; additionally, slow and fast gamma preferentially synchronize with different phases of theta, further supporting the hypothesis of their distinctive functions (evidence for this hypothesis reviewed in Colgin (2015)).

Generally, gamma oscillations are thought to play a role in communication between cells in distributed brain regions, particularly communication that requires fast organization of neuronal assemblies, such as memory formation and retrieval (Colgin and Moser, 2010). Gamma oscillations (40-120 Hz) in the hippocampus were shown to couple areas CA1 and CA3 during memory retrieval (Montgomery and Buzsaki, 2007). Low gamma oscillations (44-64 Hz) in the hippocampus were also shown to predict successful memory formation in humans (Sederberg et al., 2007).

In the amygdala, a decrease in 70-120 Hz gamma was observed during periods of safety during fear conditioning (Stujenske et al., 2014), as well as an increase in 30-80 Hz gamma (Courtin et al., 2014) in the BLA during CS+ presentation, showing that different types of gamma oscillations may play different roles in fear memory.

Courtin et al. have found an enhancement in 30-80 Hz gamma oscillations in the basolateral amygdala following fear conditioning in mice. Gamma waves were enhanced in the retrieval phase (particularly for CS+ presentation), as well as in the extinction phase. Persistence of gamma waves in extinction was also a predictor of spontaneous fear memory recovery after it has been extinguished, further implicating them in memory retrieval. Gamma oscillations in the amygdala were also enhanced for negative stimuli presentation, as compared to neutral stimuli, suggesting that amygdala might bind the perceptual visual representations with the emotional component of the stimulus (Oya et al., 2002).

1.2.3 Neural synchronization and cross-frequency coupling

Brain regions can communicate via synchronization of firing in certain frequency ranges, forming neural assemblies. This synchronization can be split into local (such as communication between subregions in a region) and long-range (communication between regions or across hemispheres). Findings from synchronizations in the theta or in the gamma range have been discussed above, but synchronization can also occur across frequencies via cross-frequency coupling (CFC). There are two types of coupling: phase-phase and phase-amplitude. In the former case, the two frequencies have aligned phases, while in the latter case, the phase of one frequency modulates the power of another.

Theta and gamma frequencies are often observed in same or neighbouring brain regions, and they also interact with each other via coupling. Theta waves are slower than gamma, and several (4 to 8) gamma cycles occur within one theta cycle. This allows for ordered representation of information via preferential firing at certain phases in the gamma and theta cycles, forming a theta-gamma neural code (Lisman and Jensen, 2013). Theta-gamma phase-phase coupling has been shown to increase during working memory tasks in the human hippocampus (Chaieb et al., 2015) and theta-gamma phase-amplitude coupling increases during associative learning in the rat hippocampus (Tort et al., 2009).

During fear conditioning, the coupling of fast gamma oscillations has been found to be functionally relevant, with gamma waves in the basolateral amygdala (BLA) coupling to theta in the same region during CS+ presentation and coupling to mPFC theta waves during CS- in rodents (Stujenske et al., 2014).

1.3 Intracranial electroencephalography

Intracranial electroencephalography (iEEG) is an invasive electrophysiological method used to measure brain activation. Intracranial EEG provides a valuable tool due to its high signal-to-noise ratio compared to EEG (in which signals have to pass through multiple tissues before they reach the scalp electrode, distorting the signal), as well as its high spatial resolution and the ability to capture signal from subcortical structures (Buzsáki et al., 2012).

This method also has disadvantages – due to its invasive nature, it is mostly performed due to clinical necessity in epilepsy patients, and therefore, considerations need to be made for epileptic activity and artefacts, as well as avoiding data from epileptogenic areas. The fact that placement is mainly based on clinical necessity also ignores many areas of the brain, providing a limited view of brain activity. Additionally, these recordings are often performed in medical settings, as opposed to laboratory conditions, which leads to less control for external variables such as power line noise or subjects' attention to the experiment. General considerations for iEEG recordings include making sure the data is gathered from non-epileptogenic regions of the brain, as well as ensuring that the results can be reproduced in several subjects and that the observations are not contrary to findings in studies of healthy subjects (Lachaux et al., 2012; Parvizi and Kastner, 2018).

Despite the limitations, intracranial EEG recordings provide a unique view of brain activity, unattainable with methods such as EEG or ECoG (grids on the cortical surface), and are the most suitable method of examining subcortical oscillatory activity.

1.4 Models of fear learning

Various models have been developed to quantitatively describe human learning and inference. For classical conditioning, the most prominent models are the Rescorla-Wagner model and the Pearce-Hall model.

The Rescorla-Wagner (RW) model describes conditioning in terms of the strength of the association between CS and US, with the strength being modulated by the effectiveness of the US and the associative strength of all stimuli present. In it, associative learning depends on the difference between expected US and presented US. This model accounts for some important phenomena in fear conditioning, such as blocking. Blocking refers to the ability of a stimulus A to block the learning of the association of a stimulus B with a US, if stimulus A had been previously paired with the same US and it is presented simultaneously with B (Rescorla and Wagner, 1972). However, this model is unable explain many other phenomena in conditioning, such as spontaneous reinstatement of the conditioned response or latent inhibition. Latent inhibition is a phenomenon in fear conditioning, in which

prior non-reinforced exposure to the CS impairs a future CS-US association (Miller et al., 1995).

The Pearce-Hall (PH) model posits that establishing the association between the CS and US depends on the associability of the CS, where the associability depends on how well it predicts the US — less accurate predictors lead to further learning. The PH model explains some phenomena that the RW model was unable to explain, such as latent inhibition, since the changing associability of CS due to its presentation in the PH model accounts for it. Nevertheless, there are still phenomena that the PH model is unable to account for, such as changing associability of a stimulus by presenting it in a novel context or how surprising events after a trial affect learning during the trial (Pearce and Hall, 1980).

In contrast with previous reinforcement learning models, learning models can also be based on Bayesian statistics, which differ from the frequentist approach to statistics by incorporating the beliefs of the observer about the state of the world. An inference about an event is made based on current observations and the prior beliefs about the probability of the event occurring, and the reliability of beliefs is also taken into account. A feature of Bayesian models is that they represent the uncertainty in beliefs with a distribution, rather than having a single value for a parameter as in reinforcement learning models (such as the RW or PH model). Gershman and Niv (2010) have proposed that Bayesian learning, which involves making inferences about the structure of the task based on observations and uncertainty, is more consistent with how learning might occur in the real world.

Bayesian models have been applied to human learning and perception: in sensorimotor learning, subjects were shown to combine previous information and current observations in a way that reflected a Bayesian strategy (Körding and Wolpert, 2004), and in reward learning, humans combined prior and subsequent information while incorporating the volatility of the source of the information into their estimate (Behrens et al., 2007).

The Bayes' Theorem, used as an update rule for the beliefs, is stated as follows:

$$P(A|B) = \frac{P(B|A) * P(A)}{P(B)} \tag{1.1}$$

In equation 1.1, $P(A|B)$ is the probability of event A given that B has already occurred (the posterior), whereas $P(B|A)$ is the probability of B given A. $P(A)$ and $P(B)$ represent the probability of observing event A and event B independently.

A probabilistic learning model that implements Bayes' Theorem as an update rule was previously applied to psychophysiological data in fear conditioning and was shown to capture the dynamics better than classical models (Tzovara, in press). This model is described below.

1.4.1 Beta-binomial model of fear learning

This probabilistic model of fear learning assumes that subjects represent the associations between CS and US as Bernoulli distributions at each time point t — $Bernoulli(\theta_t^{CS})$, and that the probabilities of US are independent between trials. The distribution of the belief about these associations is a Beta distribution, since it is the conjugate prior of the Bernoulli distribution —$Beta(\alpha_t^{CS}, \beta_t^{CS})$. The mean of the prior distribution represents the expected outcome, and this distribution is continuously updated using the observed CS and the previous outcomes (detailed in Methods).

There are several variables in this model that can be related to physiological measures or other correlates of fear conditioning. In Tzovara et al. (2018a), pupil size correlated with the US expectation in human fear conditioning and the skin conductance response correlated with a combination of uncertainty and the US expectation. In the present study, the relationship between oscillations and expected outcome was investigated.

1.5 Summary and goals

The amygdala and the hippocampus show oscillatory activity in fear conditioning, with various findings across species. The goal of this study was to investigate theta and gamma oscillations in the human hippocampus and amygdala during fear conditioning in order to gain a better understanding of their contribution to fear learning. Using an invasive electrophysiological method of recording provided an excellent view of the activity of these structures, as well as a way to relate animal local field potential findings to human fear conditioning. Additionally, an established learning model that was shown to capture psychophysiological dynam-

ics of fear learning was applied to the data with the goal of understanding the role of neural oscillations in computing the expectation of threat.

Methods

2.1 Experimental design

The experiment consisted of a standard differential fear conditioning paradigm. In the task, human subjects were asked to fixate their gaze on a cross in the center of a display and were presented with either a CS+ (signalling the onset of the aversive stimulus) or CS- (safety cue) for 4 seconds, with the US starting 3.5 seconds after CS onset in 50% of CS+ trials (see figure 2.1). Conditioned stimuli were centrally presented on a computer monitor, positioned at the patient's bed. The Subjects were also asked to press a key according to the stimulus color, and their responses and response times were recorded.

The task was implemented using Cogent software (version 2000; Wellcome Laboratory of Neurobiology, UCL). The unconditioned stimulus was a burst of white noise (95 dB, 0.5 s). The conditioned stimulus was a red or blue square, randomized between subjects and the inter-trial intervals ranged from 11 to 13 seconds. Each block consisted of 80 trials, the average number of trials per patient before exclusions ($\pm$ SD) is 91.6 $\pm$ 53 and the average number of blocks ($\pm$ SD) is 1.6 $\pm$ 0.5 (the average number of excluded trials is reported in Table 2.1).

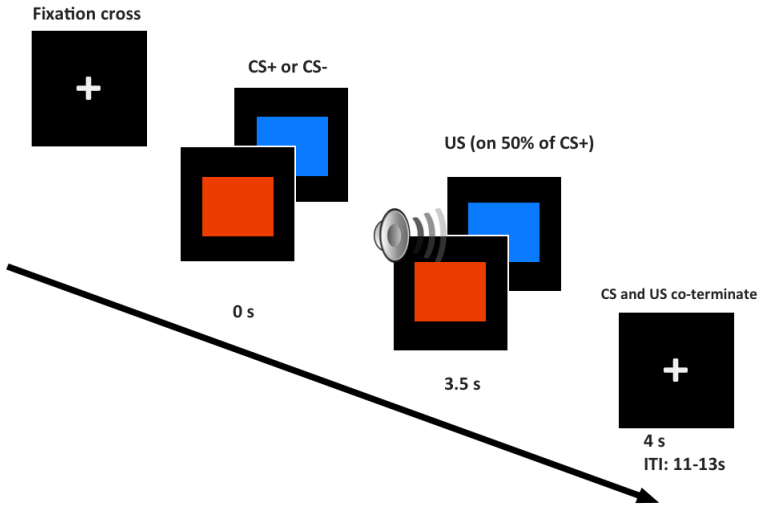

Figure 2.1: **Experimental setup.** A schematic of the experimental setup, showing the fixation cross and the arrival times of the CS and the US.

2.2 Participants

The iEEG data was gathered at UniversitätsSpital Zürich in six patients aged 17 to 56 (mean age $\pm$ SD = 37.6 $\pm$ 13.5 years, two females) with stereotactically implanted depth electrodes. All patients had temporal lobe epilepsy and electrode placement was based on clinical necessity (average number of electrodes per subject $\pm$ SD = 52.5 $\pm$ 17.4). A T1 weighted MRI scan was obtained prior to the electrode implantation, as well as a CT scan with 1 mm resolution after the operation.

2.3 Data acquisition

During the experiment, LFP recordings from depth electrodes were obtained at a sampling frequency of 4000 Hz using the ATLAS recording system and band-pass filtered between 0.5 and 1000 Hz using Neuralynx acquisition software (Neuralynx, USA). The LFP were recorded against a common intracranial reference. Single unit recordings were obtained simultaneously, but not analysed in the context of the present thesis.

2.4 Data preprocessing

Data were preprocessed using Fieldtrip and SPM12 software packages (Oostenveld et al., 2011; Litvak et al., 2011) for Matlab (version 9.1.0, Mathworks, Natick, MA, USA). After converting the LFP data from the native Neuralynx format into SPM format, a 4th order Butterworth zero-phase low-pass filter (with a 120 Hz cut-off) was applied to remove possible high-frequency epileptic artefacts. The data was down-sampled to 240 Hz (since the highest frequency of interest is 120 Hz) for ease of subsequent processing.

To account for the stimulus presentation time, data was split into segments corresponding to [-1; 6] seconds around each CS, with the 1 s prestimulus time used as baseline for subsequent time-frequency decomposition rescaling. The event markers recorded with Neuralynx and the markers sent by the software were compared against each other, with any extraneous Neuralynx pseudo-markers being excluded.

Data was referenced to the white matter contacts on each stripe (choice of reference is detailed in Subsection 2.4.1). Visual artefact rejection was performed manually using the `ft_visual_artefact_rejection` function in FieldTrip. Trials with epileptic artefacts such as sharp spikes with a high amplitude or high amplitude rhythmic activity (indicating ictal or interictal activity) were rejected and not included in the analysis. After artefact rejection and assessing the quality of the recording, one patient was excluded due a technical error during the experiment leading to the absence of paired CS+. Table 2.1 contains the number of trials before and after exclusion for each patient.

2.4.1 Signal reference

The choice of a reference signal in iEEG processing can impact the resulting data (Lachaux et al., 2012; Mercier et al., 2017). Ideally, the signal used as a reference should be as neutral as possible to avoid potential contamination (Mercier et al., 2017). Most commonly used reference methods have particular disadvantages: for instance, using a common average reference can spread local high frequency activity over all electrodes. Commonly used bipolar reference also introduces potential issues: the logic of using a bipolar reference dictates that noise at two neighbouring sources will be cancelled out by subtracting the two, but if the

time-series of the two adjacent electrodes are identical in amplitude, the activity of interest will also be cancelled out (Zaveri et al., 2006; Lachaux et al., 2012). In particular, Zaveri et al. have found that bipolar reference can result in either an introduction of unwanted activity into the signal, or the removal of common activity that is part of the phenomena under observation (in their study, theta activity in the human hippocampus was removed by a bipolar montage, while still present in the referential montage).

In the present study, both bipolar and referential montage were initially applied to the data for comparative purposes. The bipolar montage was constructed by subtracting the activity of adjacent electrodes. For the white matter montage, channels localized to the white matter (localization procedure described further in Subsection 2.4.2) were used. There were several white matter channels available per each stripe, and the time series from each of those channels was inspected for high amplitude activity that could have been conducted from other sources and would impact the resulting signal. A reference signal that is distant from the site of the recording can minimize the potential unwanted contributions (Boatman-Reich et al., 2010), so the choice of white matter channels was also influenced by the distance from the electrode of interest. While white matter itself is not completely electrically neutral (Mercier et al., 2017) and could also introduce unwanted activity from distal sites, an examination of the output from the two reference methods revealed that the signal recorded at adjacent sites was virtually identical and subtracting the two could result in complete elimination of the activity of interest. Since the bipolar reference presented a challenge in terms of resulting activity and also led to a loss of available electrodes, data from the electrodes of interest was referenced to a white matter electrode on each stripe.

2.4.2 Electrode localization

For proper analysis of LFP recordings with regards to their origin, depth electrodes needed to be localized. This was achieved using the FreeSurfer analysis suite (Fischl, 2012), SPM methods for co-registering the MR images with the CT images, and the iElectrodes open-source toolbox for localization and labelling of electrodes (Blenkmann et al., 2017). The electrodes were clustered using the co-registered scans and the iElectrodes toolbox, and labelled using the subcortical segmentation atlas available in FreeSurfer (Fischl et al., 2002). Electrode loca-

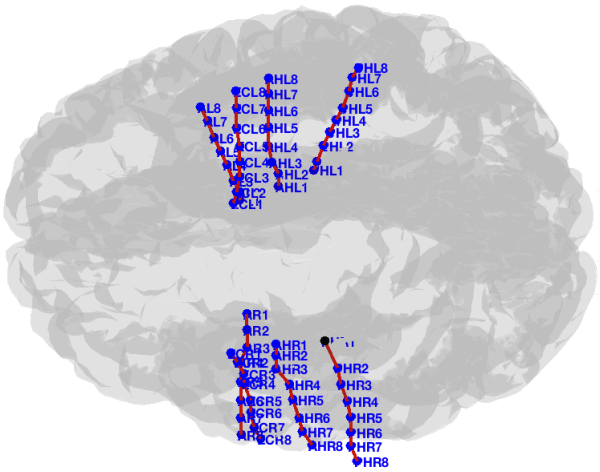

Figure 2.2: **Example of completed electrode localization.** 3D view of the reconstructed brain of one of the subjects in the study with localized electrodes in iElectrodes toolbox, dorsal view

tions were visually inspected and occasionally manually modified to account for clustering errors, and the labelling was checked by an expert in neuroanatomy to confirm the location of the electrodes of interest.

2.5 Summary of data

Table 2.1 shows a summary of all the processed data used for subsequent analyses, including the number of contacts in the amygdala and the hippocampus as well as trials excluded due to artefacts.

Patient	Electrodes	Amygdala contacts	HC contacts (anterior / posterior)	Trials before exclusion	Average trials excluded per channel
1	64	2	3 (1/2)	95	13
2	64	6	7 (5/2)	44	13
3	63	2	7 (4/3)	160	42
4	32	2	2 (2/0)	35	28
5	64	4	4 (4/0)	124	18
6	28	-	-	75	patient excluded

Table 2.1: **Summary of analyzed data** A summary of the total number of trials and contacts analyzed.

2.6 Data analysis

2.6.1 Statistical analysis

Linear mixed effects (LME) models used to analyze power and phase lag index are an extension of linear regression that incorporates both fixed and random effects. This allows us to analyze repeated-measures data and generalize over several subjects in order to describe the relationship between the response variable and the factors, while accounting for the unbalanced dataset (Keselman et al., 2001). Due to inter-subject variations such as trial number and channel location, as well as the existence of missing data due to artefact rejection, LME models were chosen as the main statistical method of analysis.

Assessing the significance in linear-mixed effects models is not straightforward, however, a literature search suggested that the most accurate method of obtaining p-values from such models is fitting the model using restricted maximum likelihood estimation and using the Satterthwaite approximation for the degrees of freedom (Luke, 2017). This was achieved using the nlme package for R (Pinheiro et al., 2014). Fitted values were plotted using the `predict` function in the nlme package with the level parameter set to 0 (predicting population values) as seen, for example, in Figure 3.3.

Model selection

Linear mixed effect models with different random effects were compared via the Akaike Information Criterion (AIC) (Akaike, 1974). AIC is a value that provides a means of comparing several models by supplying a measure of relative model fit that is penalized according to the number of parameters, therefore controlling the trade-off between model fit and model complexity. The relative likelihood of minimizing the information loss in model x compared to the model with the minimum AIC is calculated as follows:

$$Relative\ likelihood = exp(\frac{AIC_{min} - AIC_x}{2}) \tag{2.1}$$

The AIC value for the LME model with the $1|Subject/Channel$ random effect was the lowest for every analysis, with substantial relative likelihood differences with other models, prompting the usage of this model. Other models used $1|Subject$ and $1|Channel$ random effects. The $1|Subject/Channel$ random effect nests the Channel effect within the Subject effect, which is appropriate for the data, considering that the channel number in different patients may not correspond to the same location, so the effect of the channel needed to be controlled for within every subject.

Corrections for multiple comparisons

Data from EEG recordings is multi-dimensional and the signal is evaluated at many frequencies and time points. This leads to the multiple comparison problem, since the large number of inferences increases the potential number of false positives.

The random label permutation test with cluster correction allows us to control the multiple comparison problem. During the test, n random permutations of the condition labels (CS+ and CS-) for each trial within a subject are performed, with a statistical test (such as a t-test) applied to each dataset with permuted labels. The test statistic is calculated for each of these permutations and a distribution of test statistics is made (Maris and Oostenveld, 2007). After the test statistic for the permutations are calculated, cluster correction is applied via a suprathreshold cluster test. In this test, the data is initially thresholded at $\alpha = 0.05$, and the test statistic within each resulting cluster is added up to get the cluster value. A

distribution of all the cluster values is generated, and the significance of the original clusters is determined using the distribution, comparing the original clusters with the largest permutation clusters at $\alpha = 0.05$. The n of permutations was set at 1000, which allows a sufficient signal-to-noise ratio without computational issues such as long processing times (Cohen, 2014, p. 463).

2.6.2 Event-related potentials analysis

Event-related potentials (ERPs) in the amygdala and hippocampus during CS presentation (time window – [0; 3.5] s) were analyzed on a between-subject level via a linear mixed effects model and corrected via the random label permutation test with cluster correction to account for the multiple comparison problem. Additionally, the ERPs during the presence and absence of the US (time window – [3.5; 4] s) were analyzed as a manipulation check to confirm the aversive nature of the US for patients.

$$Signal \sim Condition \times Time + (1|Subject/Channel) \tag{2.2}$$

2.6.3 Time-frequency analysis

To determine if CS+ presentation influenced theta and gamma activity, time-frequency decomposition of the data was performed using Morlet wavelets with 7 cycles for each frequency in the range of 1 to 120 Hz in 1 Hz steps (via SPM).

Morlet wavelets have a Gaussian shape in the time and frequency domains, and they are best suited for time-frequency computations without losing precision in either domain. The number of cycles in the Morlet wavelet represents the trade-off between precision in the two domains, with more cycles leading to a lower precision in time, but higher frequency precision (Cohen, 2014, p. 145). The resulting time-frequency data was rescaled using the `spm_eeg_tf_rescale` function in SPM using the logarithmic rescaling method, which computes the logarithmic power and baseline corrects the data using the provided baseline (1 second before the stimulus onset in this case) (FIL Methods Group et al., 2013).

Time-frequency data was exported to R version 3.4.4 (R Core Team, 2018) to perform LME model analysis. Averaged power for each frequency band between 1 and 120 Hz — theta, alpha, beta, gamma and high gamma, as defined in Khemka

et al. (2017) — was extracted for each amygdala and hippocampus contact in every subject. The definitions of the frequency bands were made with regards to previous literature, particularly for the theta band that was found to have a lower frequency in humans (Jacobs, 2013); definitions for other frequency bands were based on conventions in the field. As an exploratory analysis, linear mixed effect models were applied to low theta (1-4 Hz) and high theta (4-8 Hz).

The power in each frequency band was analyzed using the following linear mixed effects model:

$$Power \sim Condition \times Frequency\ band \times Time + (1|Subject/Channel) \quad (2.3)$$

In this equation, the relationship between power and the fixed effects (condition, frequency band and time) is modelled. $1|Subject/Channel$ represents the Subject random effect, with the Channel effect nested within the subject (to account for the variation in channels between subjects).

The following linear mixed effect model was used to analyze averaged power in each of the frequency bands of interest (theta, low gamma and high gamma).

$$Power \sim Condition \times Time + (1|Subject/Channel) \quad (2.4)$$

The data for every combination of time-point and frequency in the range of 1 to 120 Hz was exported. An LME model was fitted to the original data, as well as to the data with 1000 random permutations of the condition labels. The t- and p-values from the models on original and permuted data for each sample and frequency combination were exported to Matlab to perform the cluster-level correction in order to control the false-positive rate due to multiple comparisons.

2.6.4 Phase synchronization analysis

Phase synchronization between the amygdala and the hippocampus was also assessed. Phase lag index (PLI) is a measure used to quantify phase synchronization and, in comparison to methods such as phase coherence, is less affected by volume conduction, a common source of interference in EEG measures (Stam et al., 2007).

The data was filtered in the range of interest (theta, gamma and high gamma) using a Butterworth filter, after which the PLI was calculated for pairs of electrodes

in the hippocampus and the amygdala (ipsilateral electrodes only) for each time point t, using custom Matlab scripts and the following formula (Khemka et al., 2017):

$$PLI = \frac{1}{T}|\sum_{t=1}^{T} sign[\phi(t, hippocampus) - \phi(t, amygdala)]| \tag{2.5}$$

The PLI values were analyzed using the following linear mixed effects model :

$$PLI \sim Condition \times Time + (1|Subject/Channel) \tag{2.6}$$

Similar to the above equations 2.3 and 2.4, condition and time are the fixed effects and $1|Subject/Channel$ is the random effect.

Phase lag index was also obtained for the theta-gamma phase-phase synchronization by changing the limits of the hippocampus Butterworth filter to 30-80 Hz for low gamma and 80 to 120 Hz for high gamma. However, previous literature suggested that phase-amplitude coupling between theta and gamma was more commonly observed in fear conditioning than phase-phase coupling, so the amplitude of the gamma range trace was obtained by using the Hilbert transform, as described in Tort et al. (2010). Then, the phase lag index for the theta-filtered trace and the envelope of the gamma trace was calculated to obtain a measure of phase-amplitude coupling.

2.6.5 Beta-binomial model analysis

In the beta-binomial model, US expectation (E[θ]) is updated on every trial given previously observed trials and current observations. The expectation is calculated as follows:

$$E[\theta] = \frac{\alpha_{t-1}}{\alpha_{t-1} + \beta_{t-1}} \tag{2.7}$$

The two parameters of the distribution represent the occurrence and non-occurrence of the US. On the first trial, both α and β are equal to 1, which gives rise to uniform Beta distributions for both the CS+ and CS-. On the subsequent trials, these parameters are updated as follows:

$$\begin{cases} \alpha_{t+1}^{CS} = \alpha_t^{CS} + 1 \text{ for US+} \\ \beta_{t+1}^{CS} = \beta_t^{CS} + 1 \text{ for US-} \end{cases}$$

The trial-by-trial expectation values were used in linear mixed effects models of phase lag index and power (equations 2.8 and 2.9). Expectation values were used in place of the condition index as an independent variable.

Based on AIC, the following models were selected:

$$PLI \sim Expectation \times Time + (1|Subject/Channel) \tag{2.8}$$

$$Power \sim Expectation + (1|Subject/Channel) \tag{2.9}$$

Results

3.1 Event-related potentials

The difference between event-related potentials (ERPs) in the time between CS onset and US onset [0;3.5 s] was analyzed between the two conditions. The linear-mixed effect model revealed significant differences for condition, trial and condition over trials interactions ($p < 0.05$, after cluster-level correction), highlighted in Figure 3.1 (top). The event-related potentials between the US and no-US conditions in the amygdala were compared as a manipulation check to ensure that the unconditioned stimulus was registered by the participants. There was a significant difference between the time courses of two potentials ($p < 0.05$), highlighted in Figure 3.1 (bottom). Since the analysis of ERPs was not the main focus of the present work, comparisons were only performed in the amygdala as a manipulation check and are not discussed further.

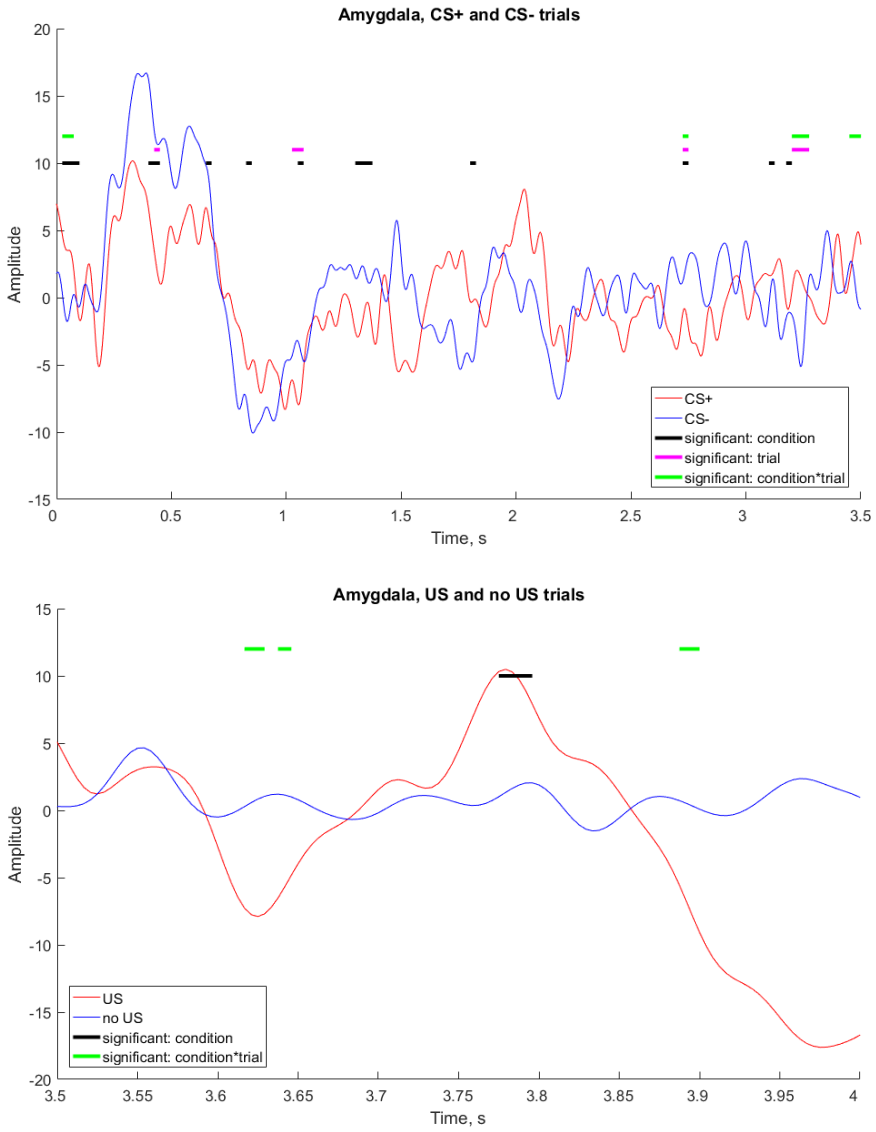

Figure 3.1: **Comparison of event-related potentials in the amygdala.** Event-related potentials between the CS onset and US onset (top) and within 2 seconds around the US presentation (bottom) were low-pass filtered at 20 Hz and analyzed via a linear mixed effect model, followed by a permutation test to control for multiple comparisons. Shown above, lines represent the grand average ($n = 5$) of all event-related potentials in the amygdala between the CS+ and CS- conditions (top) and the paired CS+ and unpaired CS+ conditions (bottom). Blocks represent significant clusters for the tested interactions from the permutation test ($p < 0.05$).

3.2 Time-frequency analysis

Time-frequency decomposition was performed between 1 and 120 Hz for all available channels in the amygdala and the hippocampus. Extracted power values for each frequency from 1 to 120 Hz at every time point were analyzed via a linear mixed effect model in equation 2.3. The significant clusters after performing the permutation test with cluster correction are shown in Figure 3.2 for each predictor.

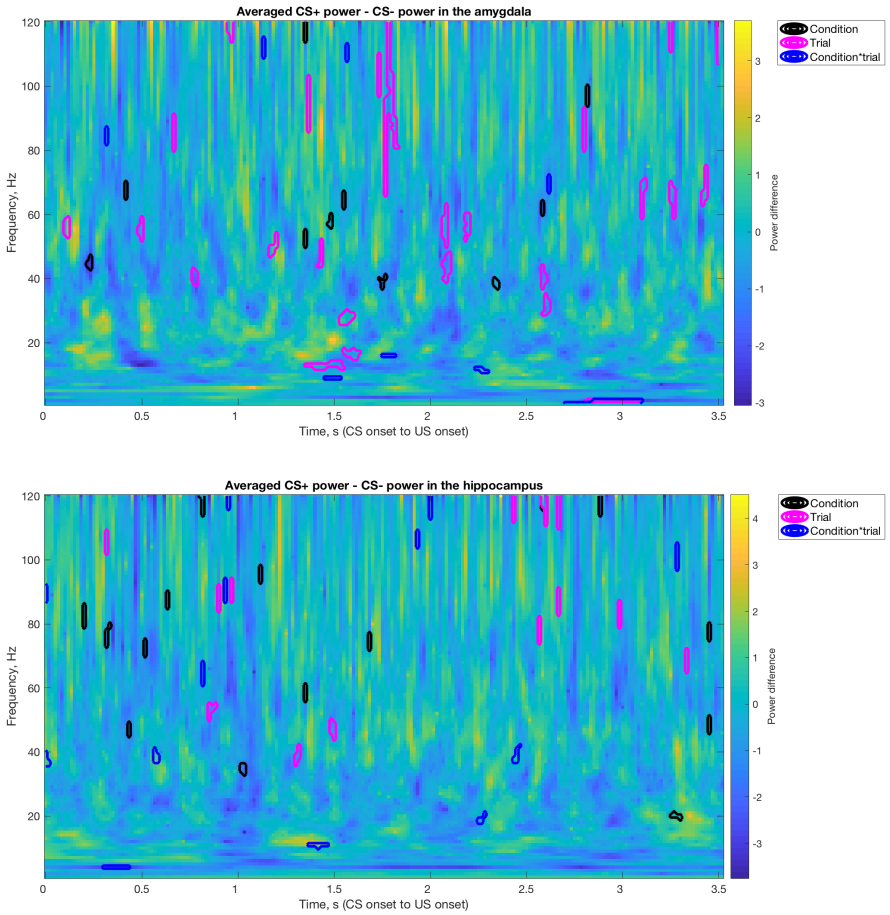

Figure 3.2: **Significant clusters from the linear mixed effect model on sample-wise time-frequency data.** Shown above is the power difference between the grand averages ($n = 5$) of CS+ and CS- responses in the amygdala and the hippocampus performed between 1 and 120 Hz via Morlet wavelets between CS onset and US onset. Contour plots represent significant clusters ($\alpha = 0.05$) for the Condition, Time and Condition×Time interactions.

Due to the fact that the LME model analysis with permutation testing and cluster correction revealed many significant clusters, a *post hoc* analysis was performed, in which the same LME model was applied to data averaged over all time points (reflecting overall activity in every frequency band) and over all frequency bands (reflecting power changes at every time point, irrespective of the frequency). This analysis was performed to determine whether there are any time points with prominent oscillatory activity or whether certain frequencies exhibit stronger overall changes between the two conditions. The overall power differences in the time domain were widespread, with no notable points of activity or time-locking to CS or US presentation. There were no significant differences for individual frequencies in case of activity averaged over all samples.

3.3 Theta power

Based on the *a priori* hypothesis that theta oscillations would differ between the CS+ and CS- conditions, theta power was investigated via a linear mixed-effect model on the power within each trial averaged between 1 and 8 Hz.

Theta band (1-8 Hz) power was averaged over every trial for each subject (n = 5) and channel. It was analyzed using the linear mixed effect model in equation 2.4. In the amygdala, no significant effects were observed. In the hippocampus, a significant effect of CS+ condition over time was observed ($p < 0.05$) (Table 3.1). Predicted values are shown in Figure 3.3.

Amygdala			**Hippocampus**		
Predictor	**T (1076)**	**p-value**	**Predictor**	**T (1607)**	**p-value**
CS+	1.0671930	0.2861	CS+	1.0441311	0.2966
Time	-0.2051367	0.8375	Time	-0.3838469	0.7011
CS+:Time	-0.5765730	0.5643	CS+:Time	-2.6577461	**0.0058**

Table 3.1: **Output of the linear mixed effect model of averaged theta band power.** Theta band power in the range of 1 to 8 Hz was averaged over single trials for every participant and channel and analyzed using a linear mixed effect model to test for effects of time and condition. A significant effect of CS+ condition over time was observed in the hippocampus (highlighted in bold above, $p < 0.05$).

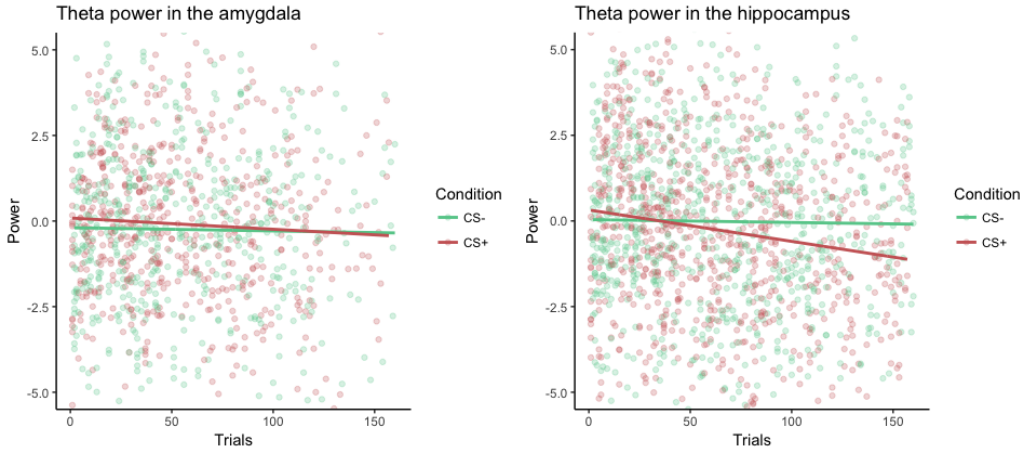

Figure 3.3: **Predicted and original averaged theta band power values.** The fitted linear mixed effect model was used to predict the theta power across all trials for the two regions. Shown above are the original values (scatterplot) and the predicted values (solid lines) for the CS+ condition (red) and the CS- condition (green).

Theta power in the hippocampus was further analysed as part of exploratory analysis to determine if hippocampal sub-regions are modulated by CS differentially. Based on previous literature, a distinction was made between anterior and posterior hippocampus, with studies showing a differential role for these regions (Fanselow and Dong, 2010; Cornwell et al., 2012) — in particular, with anxiety-like behavior being associated with the anterior hippocampus. Therefore, theta power was analysed separately for channels localised to the anterior and the posterior hippocampus. Predicted values from the analysis are shown in Figure 3.4.

A significant interaction of condition and time was found only for the anterior hippocampus, as shown in Table 3.2.

Finally, theta band power (1-8 Hz) was split into low and high theta to determine whether the chosen frequency range could have affected the results, since many studies use 4-8 Hz range for investigating the theta band in humans and primates (e.g. Sperl et al. (2018) or Taub et al. (2018)). The same linear mixed effects model used for the overall theta band was applied to data averaged in the low theta (1-4 Hz) and high theta (4-8 Hz) bands (Figure 3.5). Results from the statistical testing exhibited the same significant effects for both sub-bands as in the results from the 1-8 Hz power analysis for both the amygdala and the hippocampus.

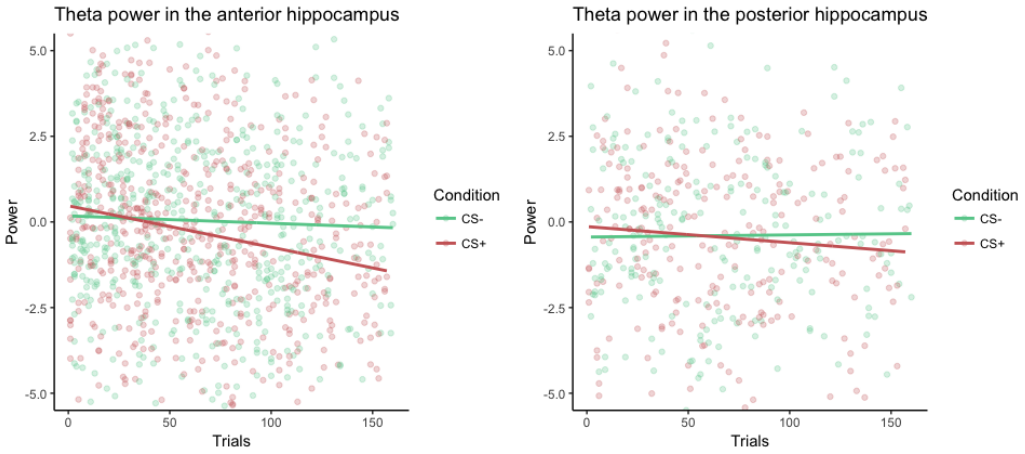

Figure 3.4: **Predicted and original averaged theta band power values in anterior and posterior hippocampus.** The fitted linear mixed effect model was used to predict the theta power across all trials for the two regions of the hippocampus. Shown above are the original values (scatterplot) and the predicted values (solid lines) for the CS+ condition (red) and the CS- condition (green).

Anterior hippocampus			**Posterior hippocampus**		
Predictor	**T (1145)**	**p-value**	**Predictor**	**T (459)**	**p-value**
CS+	0.9307733	0.3522	CS+	0.6226350	0.5338
Time	-0.8257081	0.4091	Time	0.1208703	0.9038
CS+:Time	-2.6370406	**0.0085**	CS+:Time	-0.9416705	0.3469

Table 3.2: **Output of the linear mixed effect model of averaged theta band power in two hippocampus regions.** Theta band power in the range of 1 to 8 Hz was averaged over single trials for every participant and analyzed using a linear mixed effect model to test for effects of time and condition in two regions of the hippocampus. A significant effect of CS+ condition over time was observed in the anterior hippocampus only (highlighted in bold above, $p < 0.05$).

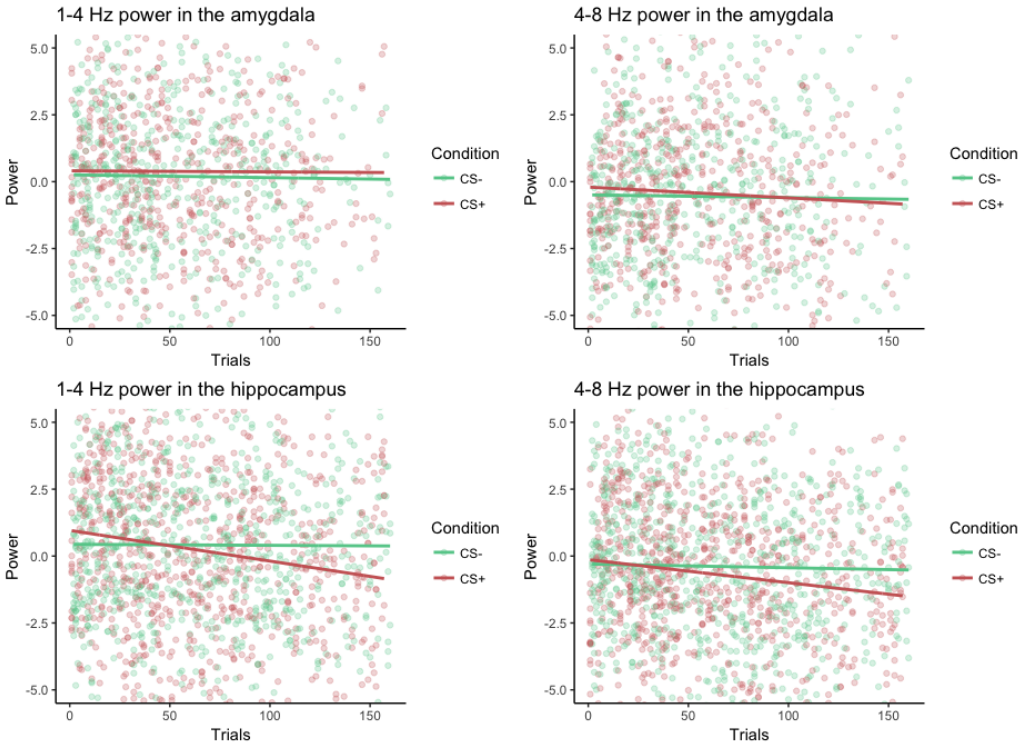

Figure 3.5: **Predicted and original averaged low and high theta power values.** The fitted linear mixed effect model was used to plot the low (1-4 Hz) and high (4-8 Hz) power across all trials in the amygdala and the hippocampus. Shown above are the original values (scatterplot) and the predicted values (solid lines) for the CS+ condition (red) and the CS- condition (green).

3.4 Gamma power

Same as with theta power, power values in the low gamma (30 to 80 Hz) and high gamma (80 to 120 Hz) range were analyzed via a linear mixed effect model. Fitted values are shown in Figure 3.6, and the output of the linear mixed effect model is shown in Table 3.3.

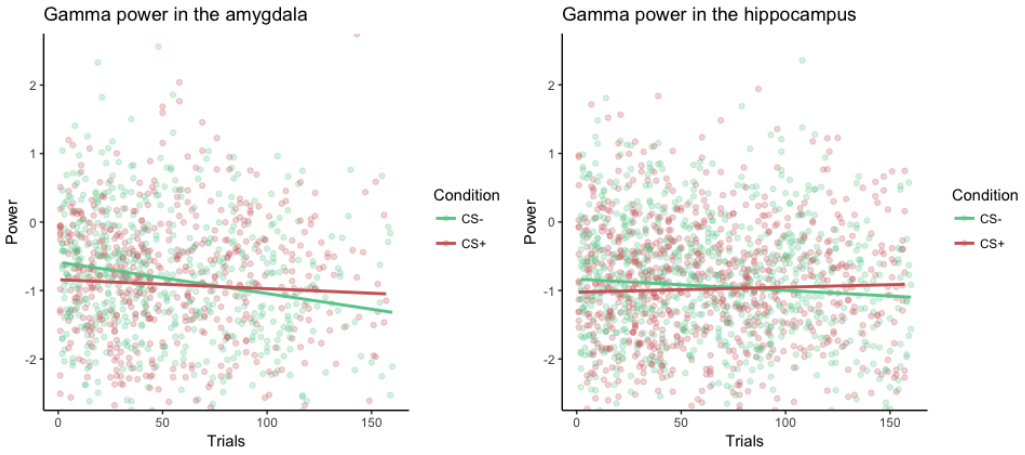

Figure 3.6: **Predicted and original averaged low gamma band power values in the amygdala and the hippocampus.** The fitted linear mixed effect model was used to plot gamma power (30 to 80 Hz) across all trials for the two regions. Shown above are the original values (scatterplot) and the predicted values (solid lines) for the CS+ condition (red) and the CS- condition (green).

A significant interaction of condition and time was found only for the amygdala.

Gamma power was also assessed in the anterior and the posterior hippocampus separately, revealing a significant effect of condition and condition over time in the anterior hippocampus only. The output of the models is summarized in Table 3.4 and the predicted values from the model are shown in Figure 3.7.

Linear mixed effect model analysis of high gamma power in the amygdala and the hippocampus did not reveal significant relationships.

Amygdala			Hippocampus		
Predictor	**T(1076)**	**p-value**	**Predictor**	**T(1607)**	**p-value**
CS+	-2.591164	**0.0097**	CS+	-1.932701	0.0534
Time	-4.136130	**0.0000**	Time	-1.776451	0.0758
CS+:Time	2.237727	**0.0254**	CS+:Time	1.844651	0.0653

Table 3.3: **Output of the linear mixed effect model of averaged gamma band power.** Gamma band power in the range of 30 to 80 Hz was averaged over single trials for every participant and channel and analysed using a linear mixed effect model to test for effects of time and condition. Significant effects of condition, time and condition over time were observed in the amygdala (highlighted in bold above, $p < 0.05$), but not in the hippocampus.

Anterior hippocampus			Posterior hippocampus		
Predictor	**T(1145)**	**p-value**	**Predictor**	**T(459)**	**p-value**
CS+	-2.275510	**0.0231**	CS+	-0.063425	0.9495
Time	-1.554286	0.1204	Time	-0.883533	0.3774
CS+:Time	2.028314	**0.0428**	CS+:Time	0.266739	0.7898

Table 3.4: **Output of the linear mixed effect model of averaged low gamma band power in two hippocampus regions.** Gamma band power in the range of 30 to 80 Hz was averaged over single trials for every participant and analyzed using a linear mixed effect model to test for effects of time and condition in two regions of the hippocampus. A significant effect of condition and condition over time was observed in the anterior hippocampus only (highlighted in bold above, $p < 0.05$).

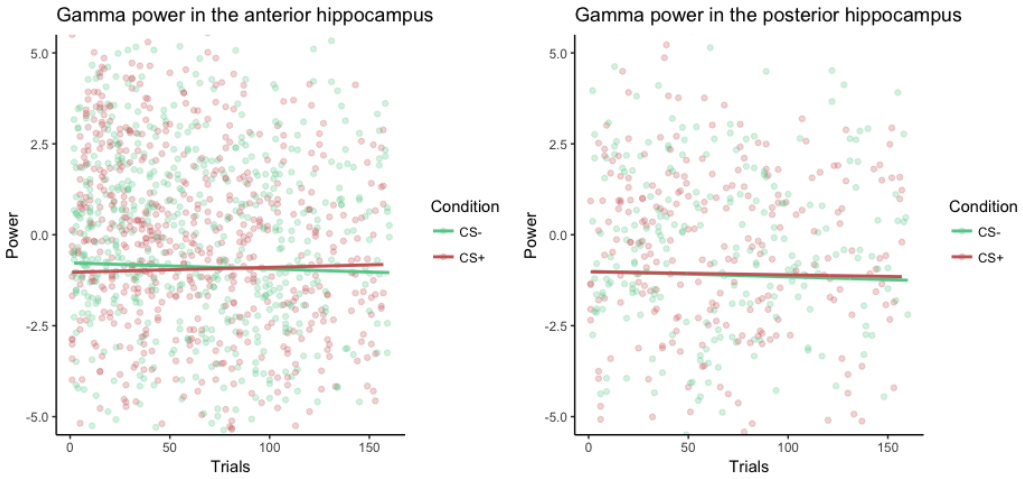

Figure 3.7: **Predicted and original averaged low gamma band power values in two hippocampus regions.** The fitted linear mixed effect model was used to plot the gamma power across all trials for the two regions. Shown above are the original values (scatterplot) and the predicted values (solid lines) for the CS+ condition (red) and the CS- condition (green).

3.5 Phase synchronization and cross-frequency coupling

Phase synchronization in the theta, low gamma and high gamma ranges between the amygdala and the hippocampus was analyzed via a linear mixed effects model, with a significant decrease in theta synchronization over time, and a significant increase over time in high gamma synchronization for CS+ condition only.

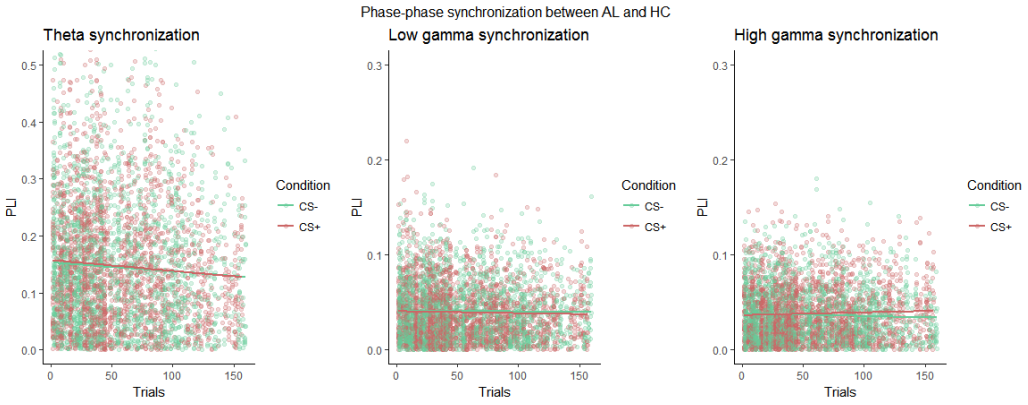

Figure 3.8: **Predicted and original phase lag index values for theta and low and high gamma range synchronization.** The fitted linear mixed effect model was used to plot the original and predicted values for the PLI between the amygdala and the hippocampus in the range of 1 to 8 Hz (left), 30 to 80 Hz (center) and 80 to 120 Hz (right). Shown above are the original values (scatterplot) and the predicted values (solid lines) for the CS+ condition (red) and the CS- condition (green).

The aforementioned phase lag index values were obtained for both ipsilateral and contralateral channels, taking into account synchronization both within the hemispheres and across the hemispheres. After restricting the analysis to ipsilateral channels only, the effect of time in theta synchronization was no longer significant ($T(2246) = -1.376$, $p = 0.1691$), same as the effect of CS+ over time in high gamma synchronization, though a trend remained ($T(2246) = 1.693$, $p = 0.09$).

Phase-phase synchronization and phase-amplitude synchronization between amygdala theta and hippocampus gamma and high gamma oscillations were also analysed, with no significant interactions.

Theta synchronization			Low gamma synchronization		
Interaction	**T(3966)**	**p-value**	**Interaction**	**T(3966)**	**p-value**
CS+	0.712972	0.4759	CS+	0.023210	0.9815
Time	-2.528152	**0.0115**	Time	-0.089326	0.9288
CS+:Time	-0.405526	0.6851	CS+:Time	-0.830775	0.4062

High gamma synchronization		
Interaction	**T(3966)**	**p-value**
CS+	-1.259764	0.2078
Time	-1.769698	0.0769
CS+:Time	2.613691	**0.0090**

Table 3.5: **Output of the linear mixed effect models of the theta, low gamma and high gamma synchronization.** Significant interactions at $\alpha = 0.05$ are highlighted in bold.

3.6 Beta-binomial model analysis

Trial-by-trial US expectation values from the beta-binomial fear learning model were calculated for each subject (Figure 3.9).

There was a significant relationship between hippocampal theta power and US expectation. Table 3.6 shows the summary of the model results.

Amygdala			Hippocampus		
Predictor	**T(1078)**	**p-value**	**Predictor**	**T(1609)**	**p-value**
Expectation	0.6225	0.5337	Expectation	-2.303	**0.0214**

Table 3.6: **Output of the linear mixed effect model of expectation and averaged theta band power.** The US expectation from the beta-binomial model was used in a linear mixed effect model as a variable that could modulate theta power. A significant effect of expectation was obtained for the hippocampus (highlighted in bold above, $p < 0.05$)

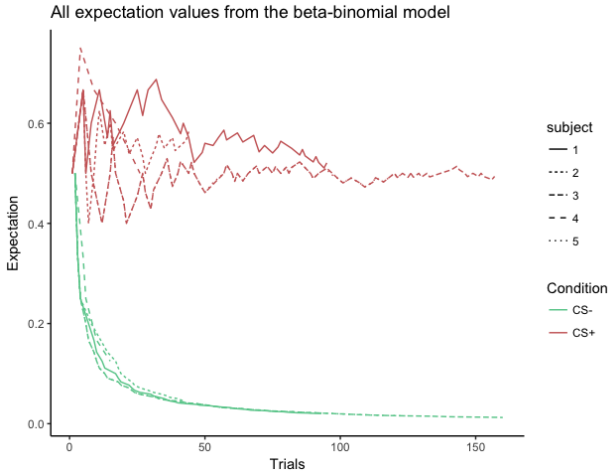

Figure 3.9: **Expectation values across trials from all subjects.** Expectation values obtained from the beta-binomial model were plotted for the CS+ (red lines) and CS- conditions (green lines), with various types of dashed lines indicating separate subjects. The lines are of different length due to the different number of trials for each subject.

There was a significant relationship between phase synchronization of amygdala and hippocampus in the theta range and US expectation. Table 3.7 shows the result of the model.

Predictor	**T (1078)**	**p-value**
Expectation	2.289251	**0.0221**
Trial	-1.412083	0.1580
Expectation:Trial	-1.786883	0.0740

Table 3.7: **Output of the linear mixed effect model of expectation and the phase synchronization in the theta range** Similarly to the above model, the expectation was used in a model of theta-range phase synchronization between the amygdala and the hippocampus. There was a significant effect of expectation on the phase lag index (highlighted in bold above, $p < 0.05$)

Discussion

In this thesis, I have investigated the role of theta and gamma oscillations as well as their synchronization during fear conditioning in humans. Section 4.1 summarizes the main findings of this study, and Sections 4.2 and 4.3 provide a critical discussion of the findings in light of previous literature in this area and potential limitations. Sections 4.4 and 4.5 outline conclusions and suggestions for future research directions based on the present results.

4.1 Summary of main results

In the time-frequency domain, cluster correction revealed multiple significant clusters in different bands, as shown in Figure 3.2, so *post hoc* analyses on data averaged over frequencies and over time were performed and corrected on the cluster level. Analyzing the overall power levels averaged over all frequency bands showed that the effects were widely distributed in time and not time-locked to stimulus presentation. There were no significant results within frequency bands for data averaged over all timepoints, which could result from smearing of activity due to averaging in the time domain.

The widespread activity and the small size of clusters could be due to several factors. For instance, while the electrode locations were checked to confirm they are in the region of interest (e.g. amygdala), they were not separated into subregions such as central or lateral nucleus of the amygdala. Therefore, averaging over data from different subregions that could have different activity during fear conditioning will lead to masking of true activity from any particular subregion. Furthermore, the SPM toolbox used for data analysis does not allow varying the amount of cycles in wavelets with frequency, which would have controlled the

temporal precision at low frequencies and frequency precision at high frequencies, giving a more consistent resolution in the time-frequency domain across a large range of frequencies.

Linear mixed-effects model analysis has shown a significant decrease in averaged theta power over time for CS+ trials in the hippocampus, which was significant only in the anterior hippocampus, and no change in the amygdala. In terms of gamma oscillations, there was a significant increase in 30-80 Hz range power over time for CS+ trials in both the amygdala and the hippocampus. There were no significant condition differences in theta range synchronization between these two regions, but overall theta synchronization decreased with time for both conditions, and synchronization in the high gamma range increased for CS+ only.

There was a significant relationship between expectation from the beta-binomial fear learning model and hippocampal theta power, as well as between the expectation values and phase synchronization in the theta range between the amygdala and the hippocampus. Analysis of the relationship between theta power in the hippocampus and expectation showed that low theta power corresponds to high expectation of the US and vice versa. In contrast, higher theta phase lag index values correlated with higher expectation.

4.2 Comparison with previous literature

4.2.1 Animal studies

In rodents, theta oscillations (4-8 Hz) were generally found to be elevated during CS+ presentation (Seidenbecher et al., 2003; Lesting et al., 2011; McHugh et al., 2014; Likhtik et al., 2014; Karalis et al., 2016), although Karalis et al. (2016) suggest that 4 Hz oscillations are associated directly with freezing behavior and not stimulus processing, and in Seidenbecher et al. (2003), this increase is only seen at 24 hours after conditioning. A decrease in theta oscillations was observed in the present study, contrary to several results in rodents, and the observed behavior of theta oscillations may reflect a difference in the process of fear acquisition in these species, further discussed in Subsection 4.2.2.

In terms of gamma oscillations, Courtin et al. (2014) have found an increase in low gamma power (30 to 80 Hz) in the amygdala following CS+ presentation during retrieval, while Stujenske et al. (2014) have observed a decrease in fast gamma

power in BLA during CS- presentation. In the present study, no changes in the high gamma (80 to 120 Hz) range were observed, but there was a significant difference between low gamma oscillations for the CS+ and CS- conditions over time with am increase in low gamma power compared to CS- presentation. In Courtin et al. (2014), the increase in gamma oscillations is attributed to a possible mechanism of encoding of fear memories, in which the amygdala communicates with other regions of the brain by synchronizing in the gamma range. However, examining the phase-phase synchronization between the amygdala and the hippocampus in the gamma range revealed no significant effects and low overall values, although the amygdala may synchronize with other regions not included in this study — for example, Bauer et al. (2007) found synchronization between the amygdala and rhinal cortices in the gamma range during a trace conditioning task in cats.

Stujenske et al. (2014) have found increased coupling between theta and fast gamma within the BLA during CS+ presentation and Lesting et al. (2011) have shown increased theta correlation between CA1 and LA during early retrieval, with lower correlation during late retrieval sessions. In the present study, no condition differences in synchronization were observed, although there was a decrease in synchronization for both conditions over time. However, Seidenbecher et al. (2003) have shown that theta range synchronization between the amygdala and the hippocampus is evident only for long-term memory retrieval in mice (e.g., at 24 h after conditioning), but not for recent memory retrieval. If similar synchronization dynamics are applicable to humans, this would help explain the absence of condition differences in theta range synchronization in the present study, since the experimental design allowed for examination of short-term retrieval only.

Stujenske et al. (2014) have also demonstrated increased BLA-vHPC fast gamma coupling for periods of safety (signalled by CS-), contrary to the present findings. The authors attribute this synchronization to the mediation of fear responses by the hippocampus, although Sierra-Mercado et al. (2011) have shown that deactivating vHPC leads to decreased fear responses. The difference in results could be attributed to the use of contextual fear conditioning by Stujenske et al. (2014), as compared to cue conditioning in the present study, which could give rise to different hippocampal dynamics.

Translating animal findings in fear conditioning to humans presents possible challenges (Lonsdorf et al., 2017). There are prominent differences in typical experimental paradigms across species, such as the type of CS (mostly visual for humans,

auditory or olfactory for animals), US (foot shock in animals, noise burst or shock for humans) or the type of outcome measure (freezing for rodents, psychophysiological response or verbal report for humans). All of these differences could affect the interpretation of results. Other potential confounds include the involvement of other brain areas that could affect activation in the amygdala, hippocampus and mPFC, as well as a prominent contribution of movement-related theta to rodent theta activity. Jacobs (2013) has also shown that 1-4 Hz hippocampal oscillations in humans and 4-8 Hz oscillations in rodents are functionally similar, and those oscillations are involved in both spatial and non-spatial tasks, further adding to the difficulty of directly extrapolating from rodent studies.

4.2.2 Human studies

Although not many studies of amygdalar and hippocampal oscillations in fear conditioning were conducted in humans, Tzovara et al. (2018b) have found a decrease in theta oscillations (1-8 Hz) in the amygdala during CS+ presentation using MEG. In the same study, a suppression of theta power in the hippocampus was observed, but did not reach significance after cluster correction. On the contrary, Sperl et al. (2018) have found that frontomedial theta oscillations increase during CS+ presentation, as captured by EEG, and this increase correlated with amygdala activation as shown by BOLD responses. It is important to note that since EEG captures signals at the scalp, localization of signals to subcortical structures is potentially problematic due to volume conduction and the existence of cortical generators (Cohen et al., 2011).

In terms of theta power changes in memory formation, Long et al. (2014) have found a decrease in low theta in the hippocampus using iEEG during memory encoding, a finding which is consistent with the present observations for CS+. The authors attribute this effect to an overall shift towards higher frequencies as a marker of successful memory encoding, which can be observed in the LME results of the present study (with significant low gamma power increases for the CS+ over time in the amygdala and the anterior hippocampus). These findings were also replicated using EEG in healthy participants, which supports the hypothesis that lower theta activity in iEEG is not due to possible spreading of epilepsy-related decreases in the alpha band to the theta band. Additionally, Greenberg et al. (2015) reported similar decreases in low theta oscillations in the temporal

lobe during associative memory encoding. This decrease is hypothesized to be related to the overall decrease of theta-range synchronization between regions, which enables more efficient local computations. Condition differences could be related to the overall higher salience of the threat signal as compared to the safety signal, which does not necessitate a fast defensive reaction and could have different encoding dynamics over time.

Theta power changes were also significant in the anterior hippocampus only, further supporting its role in emotional processing and fear conditioning (Fanselow and Ledoux, 1999), particularly cue conditioning. Pape and Pare (2010) demonstrated that posterior hippocampus played a role in contextual fear conditioning, but since the present experiment only utilized cues as the stimuli, the absence of its contributions is expected.

In humans, low gamma oscillations (30-80 Hz) have been linked to memory formation (Sederberg et al., 2007) and emotional memory formation in particular (Headley and Paré, 2013), which would help explain the dissociation in gamma oscillations between the CS+ and CS- observed in the present study, given that the CS+ is a threat predictor that could evoke the subjective emotional state of fear.

Tzovara et al. (2018b) have shown that theta range synchronization between the hippocampus and the amygdala increases for CS+ condition only. This increase in synchrony was interpreted as a signal of upcoming threat. However, in the present study, theta range synchronization decreased over time for both conditions, and although higher US expectation values did correlate with increased synchronization, the absence of condition differences in synchronization means that it cannot be a predictor of upcoming threat. A significant decrease in theta synchronization both within and between hemispheres, as compared to synchronization between the amygdala and the hippocampus in the same hemisphere supports the aforementioned hypothesis by Greenberg et al. (2015), which proposes that associative memory encoding suppresses long-range correlations with a focus on local computations.

Synchronization in the high gamma range between these two areas increased over time for CS+, which could make it a mechanism for signalling threat information; alternatively, high gamma oscillations have also been linked to increased firing rate of single neurons (Scheffer-Teixeira et al., 2013), and analyzing single

neuron activity will help determine whether this finding represents a rhythm or a contribution of extracellular spikes.

Analyzing the relationship between US expectation values from the beta-binomial model and oscillations revealed that expectation of the US modulated hippocampal theta oscillations and hippocampal-amygdalar synchrony. Boorman et al. (2016) demonstrated that BOLD activity in the hippocampus and right amygdala reflected the association strength between stimuli and rewards from a normative Bayesian learning model, although orbitofrontal cortex was found to update the stimulus-outcome associations, and the authors hypothesize that the hippocampus and amygdala could be the storage site for the associations. Following this hypothesis, increased synchronization between these two areas during US expectation could represent the retrieval of the association memory.

Higher US expectation also correlated with suppression of theta oscillations in the hippocampus. Theta oscillations in the lateral and medial frontal cortex have been previously linked to prediction errors in reinforcement learning (Cavanagh et al., 2010), and Garrido et al. (2015) have shown that theta oscillations in the vmPFC and hippocampus are involved mismatch detection, which signals unexpected changes in outcome based on past observations. Although these findings are not directly comparable with the expectation term from the beta-binomial model, they suggest a putative role for hippocampal theta oscillations in signalling changes in the environment and violations of expectation.

4.3 Limitations

In terms of limitations, the present study has several factors which could affect the results. Firstly, the amount of subjects and data is very low due to the utilized method (since iEEG is guided by clinical necessity). The electrode placement is unique for each subject, and although localization has allowed us to know the approximate location of the electrodes, inter-subject variations could still exist. Therefore, averaging over such data would smear or mask any changes in potentials or power that are spatially specific, although linear mixed effects modelling is able to account for missing data and potential differences between subjects better than t-tests.

Secondly, the trials utilized in this study are from the acquisition phase of fear conditioning, whereas most reported findings on theta and gamma oscillations in

the hippocampus and amygdala are from maintenance trials where the CS-US association is assumed to be learned. However, it is unclear exactly how fast fear learning occurs, with some animal and human studies reporting learning as fast as within one trial for specific stimuli (Haesen et al., 2017), so the later trials in this experiment could represent the maintenance phase as well.

Most animal studies also select for animals who exhibit freezing behavior or any other conditioned fear response to the CS, but in this study, no psychophysiological measures were available and selection of data by learning criteria was therefore impossible, although the significant differences between CS+ and CS- ERPs shown in Figure 3.1 reflect a difference in how the patients reacted to the two cues. The significant differences between reinforced and non-reinforced CS trials also indicate that the US presentation had an effect, despite the potential limitations due to the clinical conditions and the lower aversive nature of the US (loud noise) as opposed to the painful stimuli typically used in rodent studies, such as a foot shock. Nevertheless, selection of patients who have successfully learned the CS-US association would improve the power of the study.

The limited availability of brain regions is also a limitation, since other areas of the brain are also involved in fear conditioning and could influence the activity in the investigated regions in ways that are impossible to infer just from the activity in the amygdala and the hippocampus, so expanding the analysis to regions such as the prefrontal cortex or the entorhinal cortices will be beneficial to interpreting the behavior of oscillations in this study.

4.4 Future directions

This study opens several areas of possible future investigations: most importantly, the demonstrated theta decreases are supported by several findings in human memory formation, but have not been extensively investigated in fear conditioning. Decreases in theta power over time for the CS+ condition could represent a mechanism of fear memory encoding that is harder to detect in animals due to the contribution of theta to movement and exploration, warranting further experiments in humans.

Analysis of single-unit recordings would also be a useful potential investigation, since oscillations have been shown to organize neuronal assemblies (Jacobs et al., 2007; Buzsáki and Wang, 2012). For instance, Rutishauser et al. (2010)

have shown that coupling of single unit spikes to theta oscillations is a predictor of memory performance, and Jacobs et al. (2007) found that single neurons in the cortex and hippocampus phase lock to delta, theta and gamma oscillations, all of which support information coding in different ways. Hippocampal theta rhythm was also shown to entrain interneurons in the BLA, regulating their timing and contributing to integration of information (Bienvenu et al., 2012). Therefore, analyzing single-unit data would provide insight into the precise role of oscillations in fear conditioning and the neuronal populations that they influence.

Another important course of investigation would be an examination of prefrontal activity, since many studies have noted its wide involvement in fear conditioning and synchronization with the amygdala and the hippocampus (Adhikari et al., 2011; Sotres-Bayon et al., 2010; Likhtik and Paz, 2015; Motzkin et al., 2015). Data from the prefrontal cortex could help elucidate the relationship between the hippocampus and the amygdala, since it projects to both regions and influences their oscillations as well. However, this direction is limited due to the chosen recording method — relatively few patients have implanted electrodes in areas outside of the temporal lobe.

4.5 Conclusions

The decrease in theta power observed in this study is contrary to animal findings in fear conditioning, but is supported by human findings in episodic and associative memory formation, revealing a role of low frequency decreases in the overall fear memory encoding process. These findings contribute to the larger body of literature examining the role of oscillations in human fear conditioning, supporting the possible dissociation between the function of rodent and human theta oscillations in fear conditioning.

In terms of gamma oscillations, an increase in gamma oscillations over time may be related to successful emotional memory encoding Colgin and Moser (2010), as evidenced by the dissociation in gamma power between the two conditions. Additionally, synchronization in the theta range between the amygdala and the hippocampus was shown to decrease over time, possibly related to a decrease in overall connectivity with a focus on local computations. The increase in high gamma synchrony is not in line with this hypothesis, but without single unit data

it is hard to separate true fast gamma oscillations from increased irregular spiking activity.

Overall, the present findings support a distinct role for theta and gamma oscillations in human fear conditioning. Schroeder and Lakatos (2009) have proposed the existence of two states in the brain, characterized by the relationship between low and high frequency oscillations. The two states are the rhythmic mode, in which coupling between low and high frequencies occurs in order to facilitate task related activity; and the vigilance mode, in which low frequency oscillations are suppressed to maximize the sensitivity of the system, but gamma waves are enhanced, as they have been shown to support stimulus selection (Börgers and Kopell, 2008). The same distinction could be applied to the process of fear acquisition, with the vigilance mode being primarily active during acquisition.

The present findings elucidate the behavior of amygdalar and hippocampal oscillations with spatial and temporal precision that was not available to previous studies, and increase our understanding of oscillatory activity in memory formation. Impaired acquisition of fear has been linked to psychiatric disorders such as generalized anxiety disorder and PTSD, and knowing the oscillatory substrates of fear acquisition furthers our knowledge of the potential mechanism for these disorders.

Bibliography

A. Adhikari, M. Topiwala, and J. Gordon. Synchronized activity between the ventral hippocampus and the medial prefrontal cortex during anxiety. *Neuron*, 65 (2):257, 2010. ISSN 1097-4199. doi: 10.1016/j.neuron.2009.12.002.Synchronized.

A. Adhikari, M. A. Topiwala, and J. A. Gordon. Single units in the medial prefrontal cortex with anxiety-related firing patterns are preferentially influenced by ventral hippocampal activity. *Neuron*, 71(5):898–910, 2011. ISSN 09652140. doi: 10.1002/nbm.3066.Non-invasive.

H. Akaike. A New Look at the Statistical Model Identification. *IEEE Transactions on Automatic Control*, 19(6):716–723, 1974. ISSN 15582523. doi: 10.1109/TAC.1974.1100705.

W. H. Alexander and J. W. Brown. Medial prefrontal cortex as an action-outcome predictor. *Nature Neuroscience*, 14(10):1338–1344, 2011. ISSN 10976256. doi: 10.1038/nn.2921. URL `http://dx.doi.org/10.1038/nn.2921`.

American Psychiatric Association. *DSM-5*. American Psychiatric Association Publishing, Washington, DC, 2013. ISBN 9780890425541. doi: 10.1176/appi.books.9780890425596.744053.

M. Arruda-Carvalho and R. L. Clem. Prefrontal-amygdala fear networks come into focus. *Frontiers in Systems Neuroscience*, 9(October):1–5, 2015. ISSN 1662-5137. doi: 10.3389/fnsys.2015.00145. URL `http://journal.frontiersin.org/Article/10.3389/fnsys.2015.00145/abstract`.

N. Axmacher, M. X. Cohen, J. Fell, S. Haupt, M. Dümpelmann, C. E. Elger, T. E. Schlaepfer, D. Lenartz, V. Sturm, and C. Ranganath. Intracranial EEG

Correlates of Expectancy and Memory Formation in the Human Hippocampus and Nucleus Accumbens. *Neuron*, 65(4):541–549, 2010. ISSN 08966273. doi: 10.1016/j.neuron.2010.02.006.

E. P. Bauer, R. Paz, and D. Pare. Gamma Oscillations Coordinate Amygdalo-Rhinal Interactions during Learning. *Journal of Neuroscience*, 27(35):9369–9379, 2007. ISSN 0270-6474. doi: 10.1523/JNEUROSCI.2153-07.2007. URL `http://www.jneurosci.org/cgi/doi/10.1523/JNEUROSCI.2153-07.2007`.

T. E. J. Behrens, M. W. Woolrich, M. E. Walton, and M. F. S. Rushworth. Learning the value of information in an uncertain world. *Nature Neuroscience*, 10(9):1214–1221, 2007. ISSN 1097-6256. doi: 10.1038/nn1954. URL `http://www.nature.com/doifinder/10.1038/nn1954`.

M. A. Belluscio, K. Mizuseki, R. Schmidt, R. Kempter, and G. Buzsaki. Cross-Frequency Phase-Phase Coupling between Theta and Gamma Oscillations in the Hippocampus. *Journal of Neuroscience*, 32(2):423–435, jan 2012. ISSN 0270-6474. doi: 10.1523/JNEUROSCI.4122-11.2012.

H. Berger. Über das Elektrenkephalogramm des Menschen. *Deutsche Medizinische Wochenschrift*, 60(51):1947–1949, 1929. ISSN 14394413. doi: 10.1055/s-0028-1130334.

T. C. Bienvenu, D. Busti, P. J. Magill, F. Ferraguti, and M. Capogna. Cell-Type-Specific Recruitment of Amygdala Interneurons to Hippocampal Theta Rhythm and Noxious Stimuli In Vivo. *Neuron*, 74(6):1059–1074, 2012. ISSN 08966273. doi: 10.1016/j.neuron.2012.04.022. URL `http://dx.doi.org/10.1016/j.neuron.2012.04.022`.

A. O. Blenkmann, H. N. Phillips, J. P. Princich, J. B. Rowe, T. A. Bekinschtein, C. H. Muravchik, and S. Kochen. iElectrodes: A Comprehensive Open-Source Toolbox for Depth and Subdural Grid Electrode Localization. *Frontiers in Neuroinformatics*, 11(March):1–16, 2017. ISSN 1662-5196. doi: 10.3389/fninf.2017.00014.

D. Boatman-Reich, P. J. Franaszczuk, A. Korzeniewska, B. Caffo, E. K. Ritzl, S. Colwell, and N. E. Crone. Quantifying auditory event-related responses in

multichannel human intracranial recordings. *Frontiers in Computational Neuroscience*, 4(March):1–17, 2010. ISSN 16625188. doi: 10.3389/fncom.2010.00004.

M. Bocchio, S. Nabavi, and M. Capogna. Synaptic Plasticity, Engrams, and Network Oscillations in Amygdala Circuits for Storage and Retrieval of Emotional Memories. *Neuron*, 94(4):731–743, 2017. ISSN 10974199. doi: 10.1016/j.neuron.2017.03.022.

E. D. Boorman, V. G. Rajendran, J. X. O'Reilly, and T. E. Behrens. Two Anatomically and Computationally Distinct Learning Signals Predict Changes to Stimulus-Outcome Associations in Hippocampus. *Neuron*, 89(6):1343–1354, 2016. ISSN 10974199. doi: 10.1016/j.neuron.2016.02.014. URL `http://dx.doi.org/10.1016/j.neuron.2016.02.014`.

C. Börgers and N. Kopell. Gamma Osillations and Stimulus Selection. *Neural Computation*, 20(2005):383–414, 2008. doi: 10.1162/neco.2007.07-06-289.

G. Buzsáki and X.-J. Wang. Mechanisms of Gamma Oscillations. *Annual Review of Neuroscience*, 35(1):203–225, jul 2012. ISSN 0147-006X. doi: 10.1146/annurev-neuro-062111-150444. URL `http://www.annualreviews.org/doi/10.1146/annurev-neuro-062111-150444`.

G. Buzsáki, C. A. Anastassiou, and C. Koch. The origin of extracellular fields and currents-EEG, ECoG, LFP and spikes. *Nature Reviews Neuroscience*, 13 (6):407–420, 2012. ISSN 1471003X. doi: 10.1038/nrn3241. URL `http://dx.doi.org/10.1038/nrn3241`.

G. Buzsáki, N. Logothetis, and W. Singer. Scaling Brain Size, Keeping Timing: Evolutionary Preservation of Brain Rhythms. *Neuron*, 80(3):751–764, 2013. doi: 10.1016/j.neuron.2013.10.002.Scaling.

J. B. Caplan, J. R. Madsen, A. Schulze-Bonhage, R. Aschenbrenner-Scheibe, E. L. Newman, and M. J. Kahana. Human theta oscillations related to sensorimotor integration and spatial learning. *The Journal of neuroscience : the official journal of the Society for Neuroscience*, 23(11):4726–4736, 2003. ISSN 1529-2401. doi: 23/11/4726[pii].

J. F. Cavanagh, M. J. Frank, T. J. Klein, and J. J. Allen. Frontal theta links prediction errors to behavioral adaptation in reinforcement learning. *NeuroImage*,

49(4):3198–3209, 2010. ISSN 10538119. doi: 10.1016/j.neuroimage.2009.11.080. URL http://dx.doi.org/10.1016/j.neuroimage.2009.11.080.

L. Chaieb, M. Leszczynski, N. Axmacher, M. Hoehne, C. E. Elger, and J. Fell. Theta-gamma phase-phase coupling during working memory maintenance in the human hippocampus. *Cognitive Neuroscience*, 6(4):149–157, 2015. ISSN 17588936. doi: 10.1080/17588928.2015.1058254. URL http://dx.doi.org/10.1080/17588928.2015.1058254.

M. X. Cohen. *Analyzing Neural Time Series Data: Theory and Practice*. MIT Press, Cambridge, MA, may 2014. ISBN 978-0-262-01987-3.

M. X. Cohen, J. F. Cavanagh, and H. A. Slagter. Event-related potential activity in the basal ganglia differentiates rewards from nonrewards: Temporospatial principal components analysis and source localization of the feedback negativity: Commentary. *Human Brain Mapping*, 32(12):2270–2271, 2011. ISSN 10659471. doi: 10.1002/hbm.21358.

L. L. Colgin. Do slow and fast gamma rhythms correspond to distinct functional states in the hippocampal network? *Brain Research*, 1621:309–315, 2015. ISSN 18726240. doi: 10.1016/j.brainres.2015.01.005.

L. L. Colgin and E. I. Moser. Gamma Oscillations in the Hippocampus. *Physiology*, 25(5):319–329, 2010. ISSN 1548-9213. doi: 10.1152/physiol.00021.2010.

D. R. Collins. Differential Fear Conditioning Induces Reciprocal Changes in the Sensory Responses of Lateral Amygdala Neurons to the CS+ and CS-. *Learning & Memory*, 7(2):97–103, mar 2000. ISSN 10720502. doi: 10.1101/lm.7.2.97.

B. R. Cornwell, N. Arkin, C. Overstreet, F. W. Carver, and C. Grillon. Distinct contributions of human hippocampal theta to spatial cognition and anxiety. *Hippocampus*, 22(9):1848–1859, 2012. ISSN 10509631. doi: 10.1002/hipo.22019.

J. Courtin. Role of cortical parvalbumin interneurons in fear behaviour. *Université de Bordeaux*, 2013.

J. Courtin, N. Karalis, C. Gonzalez-Campo, H. Wurtz, and C. Herry. Persistence of amygdala gamma oscillations during extinction learning predicts spontaneous

fear recovery. *Neurobiology of Learning and Memory*, 113:82–89, 2014. ISSN 10959564. doi: 10.1016/j.nlm.2013.09.015.

H. D. Critchley, C. J. Mathias, and R. J. Dolan. Fear-conditioning in humans: the influence of awareness and arousal on functional neuroanatomy. *Neuron*, 33: 653–663, 2002.

M. Davis. The role of the amygdala in fear and anxiety. *Annu Rev Neurosci*, 15: 353–375, 1992. ISSN 0147-006X. doi: 10.1146/annurev.ne.15.030192.002033.

A. Desmedt, A. Marighetto, G. Richter-Levin, and L. Calandreau. Adaptive emotional memory: The key hippocampal-amygdalar interaction. *Stress*, 18(3): 297–308, 2015. ISSN 16078888. doi: 10.3109/10253890.2015.1067676. URL `http://dx.doi.org/10.3109/10253890.2015.1067676`.

P. Duits, D. C. Cath, S. Lissek, J. J. Hox, A. O. Hamm, I. M. Engelhard, M. A. Van Den Hout, and J. M. Baas. Updated meta-analysis of classical fear conditioning in the anxiety disorders. *Depression and Anxiety*, 32(4):239–253, 2015. ISSN 15206394. doi: 10.1002/da.22353.

J. E. Dunsmoor and R. Paz. Fear Generalization and Anxiety: Behavioral and Neural Mechanisms. *Biological Psychiatry*, 78(5):336–343, 2015. ISSN 18732402. doi: 10.1016/j.biopsych.2015.04.010. URL `http://dx.doi.org/10.1016/j.biopsych.2015.04.010`.

A. K. Engel, P. Fries, and W. Singer. Dynamic Predictions: Oscillations and Synchrony in Top-Down Processing. *Nature Reviews Neuroscience*, 2(October): 704–716, 2001. ISSN 1471-003X. doi: 10.1038/35094565.

M. S. Fanselow. Neural organization of the defensive behavior system responsible for fear. *Psychonomic Bulletin & Review*, 1(4):429–438, 1994. ISSN 10699384. doi: 10.3758/BF03210947.

M. S. Fanselow and H. W. Dong. Are the Dorsal and Ventral Hippocampus Functionally Distinct Structures? *Neuron*, 65(1):7–19, 2010. ISSN 08966273. doi: 10.1016/j.neuron.2009.11.031.

M. S. Fanselow and J. E. Ledoux. Why we think Pavlovian fear conditioning occurs in the basolateral amygdala. *Neuron*, 23:229–232, 1999. ISSN 0896-6273.

A. C. Felix-Ortiz, A. Beyeler, C. Seo, C. A. Leppla, C. P. Wildes, and K. M. Tye. BLA to vHPC inputs modulate anxiety-related behaviors. *Neuron*, 79(4): 658–664, 2013. ISSN 08966273. doi: 10.1016/j.neuron.2013.06.016.

FIL Methods Group, J. Ashburner, G. R. Barnes, C.-c. Chen, J. Daunizeau, R. Moran, R. Henson, V. Glauche, and C. Phillips. *SPM12 Manual*. 2013. ISBN 0962-1083. doi: 10.1111/j.1365-294X.2006.02813.x.

B. Fischl. FreeSurfer. *NeuroImage*, 62(2):774–781, 2012. ISSN 10538119. doi: 10.1016/j.neuroimage.2012.01.021.FreeSurfer.

B. Fischl, D. H. Salat, E. Busa, M. Albert, M. Dieterich, C. Haselgrove, A. van der Kouwe, R. Killiany, D. Kennedy, S. Klaveness, A. Montillo, N. Makris, B. Rosen, and A. M. Dale. Whole Brain Segmentation: Neurotechnique Automated Labeling of NeuroanatomicalStructures in the Human Brain. *Neuron*, 33(3): 341–355, 2002. ISSN 08966273. doi: 10.1016/S0896-6273(02)00569-X. URL `http://eutils.ncbi.nlm.nih.gov/entrez/eutils/elink.fcgi?dbfrom=pubmed{&}id=11832223{&}retmode=ref{&}cmd=prlinks{%}5Cnpapers2://publication/uuid/23BE8334-219B-4E46-AE68-C9D02B8AC109`.

P. Fries, J. H. Reynolds, A. E. Rorie, and R. Desimone. Modulation of oscillatory neuronal synchronization by selective visual attention. *Science*, 291(5508):1560–1563, 2001. ISSN 00368075. doi: 10.1126/science.1055465.

M. I. Garrido, G. R. Barnes, D. Kumaran, E. A. Maguire, and R. J. Dolan. Ventromedial prefrontal cortex drives hippocampal theta oscillations induced by mismatch computations. *NeuroImage*, 120:362–370, 2015. ISSN 10959572. doi: 10.1016/j.neuroimage.2015.07.016. URL `http://dx.doi.org/10.1016/j.neuroimage.2015.07.016`.

F. J. Gazendam, J. H. Kamphuis, and M. Kindt. Deficient safety learning characterizes high trait anxious individuals. *Biological Psychology*, 92(2):342–352, 2013. ISSN 03010511. doi: 10.1016/j.biopsycho.2012.11.006. URL `http://dx.doi.org/10.1016/j.biopsycho.2012.11.006`.

S. J. Gershman and Y. Niv. Learning latent structure: Carving nature at its joints. *Current Opinion in Neurobiology*, 20(2):251–256, 2010. ISSN 09594388.

doi: 10.1016/j.conb.2010.02.008. URL `http://dx.doi.org/10.1016/j.conb.2010.02.008`.

S. Ghosh and S. Chattarji. Neuronal encoding of the switch from specific to generalized fear. *Nature Neuroscience*, 18(1):112–120, 2015. ISSN 15461726. doi: 10.1038/nn.3888. URL `http://dx.doi.org/10.1038/nn.3888`.

R. Goutagny, J. Jackson, and S. Williams. Self-generated theta oscillations in the hippocampus. *Nature Neuroscience*, 12(12):1491–1493, 2009. ISSN 10976256. doi: 10.1038/nn.2440.

J. A. Greenberg, J. F. Burke, R. Haque, M. J. Kahana, and K. A. Zaghloul. Decreases in theta and increases in high frequency activity underlie associative memory encoding. *NeuroImage*, 114:257–263, 2015. ISSN 10959572. doi: 10.1016/j.neuroimage.2015.03.077.

K. Haesen, T. Beckers, F. Baeyens, and B. Vervliet. One-trial overshadowing: Evidence for fast specific fear learning in humans. *Behaviour Research and Therapy*, 90:16–24, 2017. ISSN 1873622X. doi: 10.1016/j.brat.2016.12.001. URL `http://dx.doi.org/10.1016/j.brat.2016.12.001`.

B. Hangya, Z. Borhegyi, N. Szilagyi, T. F. Freund, and V. Varga. GABAergic Neurons of the Medial Septum Lead the Hippocampal Network during Theta Activity. *Journal of Neuroscience*, 29(25):8094–8102, 2009. ISSN 0270-6474. doi: 10.1523/JNEUROSCI.5665-08.2009. URL `http://www.jneurosci.org/cgi/doi/10.1523/JNEUROSCI.5665-08.2009`.

D. B. Headley and D. Paré. In sync: gamma oscillations and emotional memory. *Frontiers in Behavioral Neuroscience*, 7(November):1–12, 2013. ISSN 1662-5153. doi: 10.3389/fnbeh.2013.00170.

M. W. Howard, D. S. Rizzuto, J. B. Caplan, J. R. Madsen, J. Lisman, R. Aschenbrenner-Scheibe, A. Schulze-Bonhage, and M. J. Kahana. Gamma Oscillations Correlate with Working Memory Load in Humans. *Cerebral Cortex*, 13(12):1369–1374, 2003. ISSN 10473211. doi: 10.1093/cercor/bhg084.

J. Jacobs. Hippocampal theta oscillations are slower in humans than in rodents: implications for models of spatial navigation and memory. *Philosophical*

Transactions of the Royal Society B: Biological Sciences, 369(1635):20130304–20130304, dec 2013. ISSN 0962-8436. doi: 10.1098/rstb.2013.0304.

J. Jacobs, M. J. Kahana, A. D. Ekstrom, and I. Fried. Brain Oscillations Control Timing of Single-Neuron Activity in Humans. *Journal of Neuroscience*, 27(14): 3839–3844, 2007. ISSN 0270-6474. doi: 10.1523/JNEUROSCI.4636-06.2007.

O. Jensen and L. L. Colgin. Cross-frequency coupling between neuronal oscillations. *Trends in Cognitive Sciences*, 11(7):267–269, 2007. ISSN 13646613. doi: 10.1016/j.tics.2007.05.003.

M. W. Jones and M. A. Wilson. Theta rhythms coordinate hippocampal-prefrontal interactions in a spatial memory task. *PLoS Biology*, 3(12):1–13, 2005. ISSN 15457885. doi: 10.1371/journal.pbio.0030402.

M. J. Kahana, R. Sekuler, J. B. Caplan, M. Kirschen, and J. R. Madsen. Human theta oscillations exhibit task dependence during virtual maze navigation. *Nature*, 399(6738):781–784, 1999. ISSN 00280836. doi: 10.1038/21645.

R. Kalisch. Context-Dependent Human Extinction Memory Is Mediated by a Ventromedial Prefrontal and Hippocampal Network. *Journal of Neuroscience*, 26(37):9503–9511, 2006. ISSN 0270-6474. doi: 10.1523/JNEUROSCI.2021-06.2006. URL `http://www.jneurosci.org/cgi/doi/10.1523/JNEUROSCI.2021-06.2006`.

N. Karalis, C. Dejean, F. Chaudun, S. Khoder, R. R Rozeske, H. Wurtz, S. Bagur, K. Benchenane, A. Sirota, J. Courtin, and C. Herry. 4-Hz oscillations synchronize prefrontal-amygdala circuits during fear behavior. *Nature Neuroscience*, 19 (4):605–612, 2016. ISSN 15461726. doi: 10.1038/nn.4251.

H. J. Keselman, J. Algina, and R. K. Kowalchuk. The analysis of repeated measures designs: A review. *British Journal of Mathematical and Statistical Psychology*, 54(1):1–20, may 2001. ISSN 00071102. doi: 10.1348/000711001159357.

M. A. Kheirbek, K. C. Klemenhagen, A. Sahay, and R. Hen. Neurogenesis and generalization: A new approach to stratify and treat anxiety disorders. *Nature Neuroscience*, 15(12):1613–1620, 2012. ISSN 10976256. doi: 10.1038/nn.3262.

S. Khemka, G. R. Barnes, R. J. Dolan, and D. R. Bach. Dissecting the Function of Hippocampal Oscillations in a Human Anxiety Model. *The Journal of Neuroscience*, 37(29):6869–6876, 2017. ISSN 0270-6474. doi: 10.1523/JNEUROSCI.1834-16.2017.

J. J. Kim, R. A. Rison, and M. S. Fanselow. Effects of amygdala, hippocampus, and periaqueductal gray lesions on short- and long-term contextual fear. *Behavioral Neuroscience*, 107(6):1093–1098, 1993. ISSN 07357044. doi: 10.1037/0735-7044.107.6.1093.

K. P. Körding and D. M. Wolpert. Bayesian integration in sensorimotor learning. *Nature*, 427(6971):244–247, 2004. ISSN 00280836. doi: 10.1038/nature02169.

R. Kramis, C. H. Vanderwolf, and B. H. Bland. Two types of hippocampal rhythmical slow activity in both the rabbit and the rat: Relations to behavior and effects of atropine, diethyl ether, urethane, and pentobarbital. *Experimental Neurology*, 49(1):58–85, 1975. ISSN 10902430. doi: 10.1016/0014-4886(75)90195-8.

J.-p. Lachaux, N. Axmacher, F. Mormann, E. Halgren, N. E. Crone, and C. B. Lyon. High-frequency neural activity and human cognition : Past , present and possible future of intracranial EEG research. *Progress in Neurobiology*, 98(3):279–301, 2012. ISSN 0301-0082. doi: 10.1016/j.pneurobio.2012.06.008.

B. C. Lega, J. Jacobs, and M. Kahana. Human hippocampal theta oscillations and the formation of episodic memories. *Hippocampus*, 22(4):748–761, 2012. ISSN 10509631. doi: 10.1002/hipo.20937.

J. Lesting, R. T. Narayanan, C. Kluge, S. Sangha, T. Seidenbecher, and H. C. Pape. Patterns of coupled theta activity in amygdala-hippocampal-prefrontal cortical circuits during fear extinction. *PLoS ONE*, 6(6), 2011. ISSN 19326203. doi: 10.1371/journal.pone.0021714.

E. Likhtik and R. Paz. Amygdala-prefrontal interactions in (mal)adaptive learning. *Trends in Neurosciences*, 38(3):158–166, 2015. ISSN 1878108X. doi: 10.1016/j.tins.2014.12.007. URL `http://dx.doi.org/10.1016/j.tins.2014.12.007`.

E. Likhtik, D. Popa, J. Apergis-Schoute, G. A. Fidacaro, and D. Paré. Amygdala intercalated neurons are required for expression of fear extinction. *Nature*, 454(7204):642–645, 2008. ISSN 00280836. doi: 10.1038/nature07167.

E. Likhtik, J. M. Stujenske, M. A. Topiwala, A. Z. Harris, J. A. Gordon, M. A Topiwala, A. Z. Harris, and J. A. Gordon. Prefrontal entrainment of amygdala activity signals safety in learned fear and innate anxiety. *Nature Neuroscience*, 17(1):106–113, jan 2014. ISSN 1097-6256. doi: 10.1038/nn.3582.

J. E. Lisman and O. Jensen. The Theta-Gamma Neural Code. *Neuron*, 77(6): 1002–1016, mar 2013. ISSN 08966273. doi: 10.1016/j.neuron.2013.03.007.

V. Litvak, J. Mattout, S. Kiebel, C. Phillips, R. Henson, J. Kilner, G. R. Barnes, R. Oostenveld, J. Daunizeau, G. Flandin, W. Penny, and K. Friston. EEG and MEG data analysis in SPM8. *Computational Intelligence and Neuroscience*, 2011, 2011. ISSN 16875265. doi: 10.1155/2011/852961.

N. M. Long, J. F. Burke, and M. J. Kahana. Subsequent memory effect in intracranial and scalp EEG. *NeuroImage*, 84:488–494, 2014. ISSN 10538119. doi: 10.1016/j.neuroimage.2013.08.052.

T. B. Lonsdorf, M. M. Menz, M. Andreatta, M. A. Fullana, A. Golkar, J. Haaker, I. Heitland, A. Hermann, M. Kuhn, O. Kruse, S. Meir Drexler, A. Meulders, F. Nees, A. Pittig, J. Richter, S. Römer, Y. Shiban, A. Schmitz, B. Straube, B. Vervliet, J. Wendt, J. M. Baas, and C. J. Merz. Don't fear 'fear conditioning': Methodological considerations for the design and analysis of studies on human fear acquisition, extinction, and return of fear. *Neuroscience and Biobehavioral Reviews*, 77:247–285, 2017. ISSN 18737528. doi: 10.1016/j.neubiorev.2017.02.026.

S. G. Luke. Evaluating significance in linear mixed-effects models in R. *Behavior Research Methods*, 49(4):1494–1502, 2017. ISSN 15543528. doi: 10.3758/s13428-016-0809-y.

S. Maren. Neurobiology of Pavlovian Fear Conditioning. *Annual Review of Neuroscience*, 24(1):897–931, mar 2001. ISSN 0147-006X. doi: 10.1146/annurev.neuro.24.1.897.

E. Maris and R. Oostenveld. Nonparametric statistical testing of EEG- and MEG-data. *Journal of Neuroscience Methods*, 164(1):177–190, 2007. ISSN 01650270. doi: 10.1016/j.jneumeth.2007.03.024.

J. L. McGaugh. The Amygdala Modulates the Consolidation of Memories of Emotionally Arousing Experiences. *Annual Review of Neuroscience*, 27(1):1–28, 2004. ISSN 0147-006X. doi: 10.1146/annurev.neuro.27.070203.144157.

S. B. McHugh, C. Barkus, A. Huber, L. Capitao, J. Lima, J. P. Lowry, and D. M. Bannerman. Aversive Prediction Error Signals in the Amygdala. *Journal of Neuroscience*, 34(27):9024–9033, 2014. ISSN 0270-6474. doi: 10.1523/JNEUROSCI.4465-13.2014.

M. R. Mercier, S. Bickel, P. Megevand, D. M. Groppe, C. E. Schroeder, A. D. Mehta, and F. A. Lado. Evaluation of cortical local field potential diffusion in stereotactic electro-encephalography recordings: A glimpse on white matter signal. *NeuroImage*, 147:219–232, 2017. ISSN 10959572. doi: 10.1016/j.neuroimage.2016.08.037.

M. R. Milad, G. J. Quirk, R. K. Pitman, S. P. Orr, B. Fischl, and S. L. Rauch. A Role for the Human Dorsal Anterior Cingulate Cortex in Fear Expression. *Biological Psychiatry*, 62(10):1191–1194, 2007. ISSN 00063223. doi: 10.1016/j.biopsych.2007.04.032.

M. R. Milad, S. P. Orr, N. B. Lasko, Y. Chang, S. L. Rauch, and R. K. Pitman. Presence and acquired origin of reduced recall for fear extinction in PTSD: Results of a twin study. *Journal of Psychiatric Research*, 42(7):515–520, 2008. ISSN 00223956. doi: 10.1016/j.jpsychires.2008.01.017.

E. K. Miller and J. D. Cohen. An Integrative Theory of Prefrontal Cortex Function. *Annual Review of Neuroscience*, 24(1):167–202, mar 2001. ISSN 0147-006X. doi: 10.1146/annurev.neuro.24.1.167.

R. R. Miller, R. C. Barnet, and N. J. Grahame. Assessment of the Rescorla-Wagner model. *Psychological Bulletin*, 117(3):363–386, 1995. ISSN 00332909. doi: 10.1037/0033-2909.117.3.363.

V. Miskovic, A. R. Ashbaugh, D. L. Santesso, R. E. McCabe, M. M. Antony, and L. A. Schmidt. Frontal brain oscillations and social anxiety: A cross-frequency spectral analysis during baseline and speech anticipation. *Biological Psychology*, 83(2):125–132, 2010. ISSN 03010511. doi: 10.1016/j.biopsycho.2009.11.010.

K. Mizuseki, A. Sirota, E. Pastalkova, and G. Buzsáki. Theta Oscillations Provide Temporal Windows for Local Circuit Computation in the Entorhinal-Hippocampal Loop. *Neuron*, 64(2):267–280, 2009. ISSN 08966273. doi: 10.1016/j.neuron.2009.08.037.

S. M. Montgomery and G. Buzsaki. Gamma oscillations dynamically couple hippocampal CA3 and CA1 regions during memory task performance. *Proceedings of the National Academy of Sciences*, 104(36):14495–14500, 2007. ISSN 0027-8424. doi: 10.1073/pnas.0701826104.

J. C. Motzkin, C. L. Philippi, R. C. Wolf, M. K. Baskaya, and M. Koenigs. Ventromedial prefrontal cortex is critical for the regulation of amygdala activity in humans. *Biological Psychiatry*, 77(3):276–284, 2015. ISSN 18732402. doi: 10.1016/j.biopsych.2014.02.014.

R. T. Narayanan, T. Seidenbecher, C. Kluge, J. Bergado, O. Stork, and H. C. Pape. Dissociated theta phase synchronization in amygdalo-hippocampal circuits during various stages of fear memory. *European Journal of Neuroscience*, 25(6):1823–1831, 2007. ISSN 0953816X. doi: 10.1111/j.1460-9568.2007.05437.x.

D. J. Oathes, W. J. Ray, A. S. Yamasaki, T. D. Borkovec, L. G. Castonguay, M. G. Newman, and J. Nitschke. Worry, generalized anxiety disorder, and emotion: Evidence from the EEG gamma band. *Biological Psychology*, 79(2):165–170, 2008. ISSN 03010511. doi: 10.1016/j.biopsycho.2008.04.005.

R. Oostenveld, P. Fries, E. Maris, and J.-M. M. Schoffelen. FieldTrip: Open Source Software for Advanced Analysis of MEG, EEG, and Invasive Electrophysiological Data. *Computational Intelligence and Neuroscience*, 2011:1–9, 2011. ISSN 16875265. doi: 10.1155/2011/156869.

C. A. Orsini and S. Maren. Neural and cellular mechanisms of fear and extinction memory formation. *Neuroscience and Biobehavioral Reviews*, 36(7):1773–1802, 2012. ISSN 01497634. doi: 10.1016/j.neubiorev.2011.12.014.

H. Oya, H. Kawasaki, M. a. Howard, and R. Adolphs. Electrophysiological responses in the human amygdala discriminate emotion categories of complex visual stimuli. *The Journal of neuroscience : the official journal of*

the Society for Neuroscience, 22(21):9502–9512, 2002. ISSN 1529-2401. doi: 10.1093/BRAIN/121.6.1143.

H.-C. Pape and D. Pare. Plastic synaptic networks of the amygdala for the acquisition, expression, and extinction of conditioned fear. *Physiological reviews*, 90 (2):419–63, apr 2010. ISSN 1522-1210. doi: 10.1152/physrev.00037.2009.

H. C. Pape, D. Paré, and R. B. Driesang. Two types of intrinsic oscillations in neurons of the lateral and basolateral nuclei of the amygdala. *Journal of neurophysiology*, 79(1):205–16, 1998. ISSN 0022-3077.

H. C. Pape, R. T. Narayanan, J. Smid, O. Stork, and T. Seidenbecher. Theta activity in neurons and networks of the amygdala related to long-term fear memory. *Hippocampus*, 15(7):874–880, 2005. ISSN 10509631. doi: 10.1002/hipo.20120.

D. Pare. New Vistas on Amygdala Networks in Conditioned Fear. *Journal of Neurophysiology*, 92(1):1–9, 2004. ISSN 0022-3077. doi: 10.1152/jn.00153.2004.

D. Paré and D. R. Collins. Neuronal correlates of fear in the lateral amygdala: multiple extracellular recordings in conscious cats. *The Journal of neuroscience : the official journal of the Society for Neuroscience*, 20(7):2701–10, 2000. ISSN 1529-2401.

J. Parvizi and S. Kastner. Promises and limitations of human intracranial electroencephalography. *Nature Neuroscience*, 21(April):1–10, 2018. ISSN 15461726. doi: 10.1038/s41593-018-0108-2.

I. P. Pavlov. Conditioned reflexes: An investigation of the physiological activity of the cerebral cortex, 1927. ISSN 08854173.

R. Paz, E. P. Bauer, and D. Paré. Theta synchronizes the activity of medial prefrontal neurons during learning. *Learning & memory (Cold Spring Harbor, N.Y.)*, 15(7):524–531, 2008. ISSN 1072-0502. doi: 10.1101/lm.932408.

J. M. Pearce and G. Hall. A model for Pavlovian learning: Variations in the effectiveness of conditioned but not of unconditioned stimuli. *Psychological Review*, 87(6):532–552, 1980. ISSN 0033295X. doi: 10.1037/0033-295X.87.6.532.

J. Pinheiro, D. Bates, S. DebRoy, D. Sarkar, and R Core Team. nlme: Linear and nonlinear mixed effects models, 2014. URL `https://cran.r-project.org/package=nlme`.

R Core Team. *R: A Language and Environment for Statistical Computing*. Vienna, Austria, 2018. URL `http://www.r-project.org/`.

S. Rachman. The return of fear: Review and prospect. *Clinical Psychology Review*, 9(2):147–168, 1989. ISSN 02727358. doi: 10.1016/0272-7358(89)90025-1.

R. A. Rescorla and A. R. Wagner. A theory of Pavlovian conditioning: Variations in the effectiveness of reinforcement and nonreinforcement. *Classical Conditioning II Current Research and Theory*, 21(6):64–99, 1972. ISSN 19416016. doi: 10.1101/gr.110528.110.

M. T. Rogan, U. V. Staubli, and J. E. LeDoux. Fear conditioning induces associative long-term potentiation in the amygdala. *Nature*, 390(6660):604–607, 1997. ISSN 00280836. doi: 10.1038/37601.

U. Rutishauser, I. B. Ross, A. N. Mamelak, and E. M. Schuman. Human memory strength is predicted by theta-frequency phase-locking of single neurons. *Nature*, 464(7290):903–907, 2010. ISSN 00280836. doi: 10.1038/nature08860. URL `http://dx.doi.org/10.1038/nature08860`.

M. J. Sanders, B. J. Wiltgen, and M. S. Fanselow. The place of the hippocampus in fear conditioning. *European Journal of Pharmacology*, 463(1-3):217–223, 2003. ISSN 00142999. doi: 10.1016/S0014-2999(03)01283-4.

R. Scheffer-Teixeira, H. Belchior, R. N. Leao, S. Ribeiro, and A. B. L. Tort. On High-Frequency Field Oscillations (>100 Hz) and the Spectral Leakage of Spiking Activity. *Journal of Neuroscience*, 33(4):1535–1539, 2013. ISSN 0270-6474. doi: 10.1523/JNEUROSCI.4217-12.2013. URL `http://www.jneurosci.org/cgi/doi/10.1523/JNEUROSCI.4217-12.2013`.

C. E. Schroeder and P. Lakatos. The gamma oscillation: Master or slave? *Brain Topography*, 22(1):24–26, 2009. ISSN 08960267. doi: 10.1007/s10548-009-0080-y.

P. B. Sederberg, A. Schulze-Bonhage, J. R. Madsen, E. B. Bromfield, D. C. McCarthy, A. Brandt, M. S. Tully, and M. J. Kahana. Hippocampal and neocortical gamma oscillations predict memory formation in humans. *Cerebral Cortex*, 17 (5):1190–1196, 2007. ISSN 10473211. doi: 10.1093/cercor/bhl030.

C. Sehlmeyer, U. Dannlowski, S. Schöning, H. Kugel, M. Pyka, B. Pfleiderer, P. Zwitserlood, H. Schiffbauer, W. Heindel, V. Arolt, and C. Konrad. Neural correlates of trait anxiety in fear extinction. *Psychological Medicine*, 41(4):789–798, 2011. ISSN 00332917. doi: 10.1017/S0033291710001248.

T. Seidenbecher, T. R. Laxmi, O. Stork, and H. C. Pape. Amygdalar and Hippocampal Theta Rhythm Synchronization During Fear Memory Retrieval. *Science*, 301(5634):846–850, aug 2003. ISSN 0036-8075. doi: 10.1126/science.1085818.

D. Sevenster, R. M. Visser, and R. D'Hooge. A translational perspective on neural circuits of fear extinction: Current promises and challenges. *Neurobiology of Learning and Memory*, 155(June):113–126, 2018. ISSN 10959564. doi: 10.1016/j.nlm.2018.07.002. URL `https://doi.org/10.1016/j.nlm.2018.07.002`.

D. Sierra-Mercado, N. Padilla-Coreano, and G. J. Quirk. Dissociable roles of prelimbic and infralimbic cortices, ventral hippocampus, and basolateral amygdala in the expression and extinction of conditioned fear. *Neuropsychopharmacology*, 36(2):529–538, 2011. ISSN 0893133X. doi: 10.1038/npp.2010.184.

F. Sotres-Bayon, G. J. Quirk, P. Fomby, and A. J. Cherlin. Prefrontal control of fear: more than just extinction. *Current Opinion in Neurobiology*, 20(2): 231–235, 2010. ISSN 1878-5832. doi: 10.1016/j.conb.2010.02.005.Prefrontal.

M. F. J. Sperl, C. Panitz, I. M. Rosso, D. G. Dillon, P. Kumar, A. Hermann, A. E. Whitton, C. Hermann, D. A. Pizzagalli, and E. M. Mueller. Fear Extinction Recall Modulates Human Frontomedial Theta and Amygdala Activity. *Cerebral Cortex*, 1(April):1–15, 2018. ISSN 1047-3211. doi: 10.1093/cercor/bhx353.

C. J. Stam, G. Nolte, and A. Daffertshofer. Phase lag index: Assessment of functional connectivity from multi channel EEG and MEG with diminished bias from common sources. *Human Brain Mapping*, 28(11):1178–1193, 2007. ISSN 10659471. doi: 10.1002/hbm.20346.

J. M. Stujenske, E. Likhtik, M. A. Topiwala, and J. A. Gordon. Fear and Safety Engage Competing Patterns of Theta-Gamma Coupling in the Basolateral Amygdala. *Neuron*, 83(4):919–933, 2014. ISSN 10974199. doi: 10.1016/j.neuron.2014.07.026.

Tallon-Baudry and Bertrand. Oscillatory gamma activity in humans and its role in object representation. *Trends in Cognitive Sciences*, 3(4):151–162, 1999. ISSN 1879-307X. doi: 10.1016/S1364-6613(99)01299-1.

A. H. Taub, R. Perets, E. Kahana, and R. Paz. Oscillations Synchronize Amygdala-to-Prefrontal Primate Circuits during Aversive Learning. *Neuron*, 97(2):291–298.e3, 2018. ISSN 10974199. doi: 10.1016/j.neuron.2017.11.042.

A. B. L. Tort, R. W. Komorowski, J. R. Manns, N. J. Kopell, and H. Eichenbaum. Theta-gamma coupling increases during the learning of item-context associations. *Proceedings of the National Academy of Sciences*, 106(49):20942–20947, 2009. ISSN 0027-8424. doi: 10.1073/pnas.0911331106.

A. B. L. Tort, R. Komorowski, H. Eichenbaum, and N. Kopell. Measuring Phase-Amplitude Coupling Between Neuronal Oscillations of Different Frequencies. *Journal of Neurophysiology*, 104(2):1195–1210, 2010. ISSN 0022-3077. doi: 10.1152/jn.00106.2010.

P. Tovote, J. P. Fadok, and A. Lüthi. Neuronal circuits for fear and anxiety. *Nature Reviews Neuroscience*, 16(6):317–331, 2015. ISSN 14710048. doi: 10.1038/nrn3945.

A. Tzovara, C. W. Korn, and D. R. Bach. Human Pavlovian fear conditioning conforms to probabilistic learning. *PLoS Computational Biology (in press)*, 2018a.

A. Tzovara, S. S. Meyer, J. J. Bonaiuto, A. Abivardi, R. J. Dolan, G. R. Barnes, and D. R. Bach. Neural oscillations in human hippocampus and amygdala during prediction of safety and threat. *Unpublished manuscript*, 2018b.

M. K. van Vugt, A. Schulze-Bonhage, B. Litt, A. Brandt, and M. J. Kahana. Hippocampal Gamma Oscillations Increase with Memory Load. *Journal of Neuroscience*, 30(7):2694–2699, 2010. ISSN 0270-6474. doi: 10.1523/JNEUROSCI.0567-09.2010.

H. P. Zaveri, R. B. Duckrow, and S. S. Spencer. On the use of bipolar montages for time-series analysis of intracranial electroencephalograms. *Clinical Neurophysiology*, 117(9):2102–2108, 2006. ISSN 13882457. doi: 10.1016/j.clinph.2006.05.032.